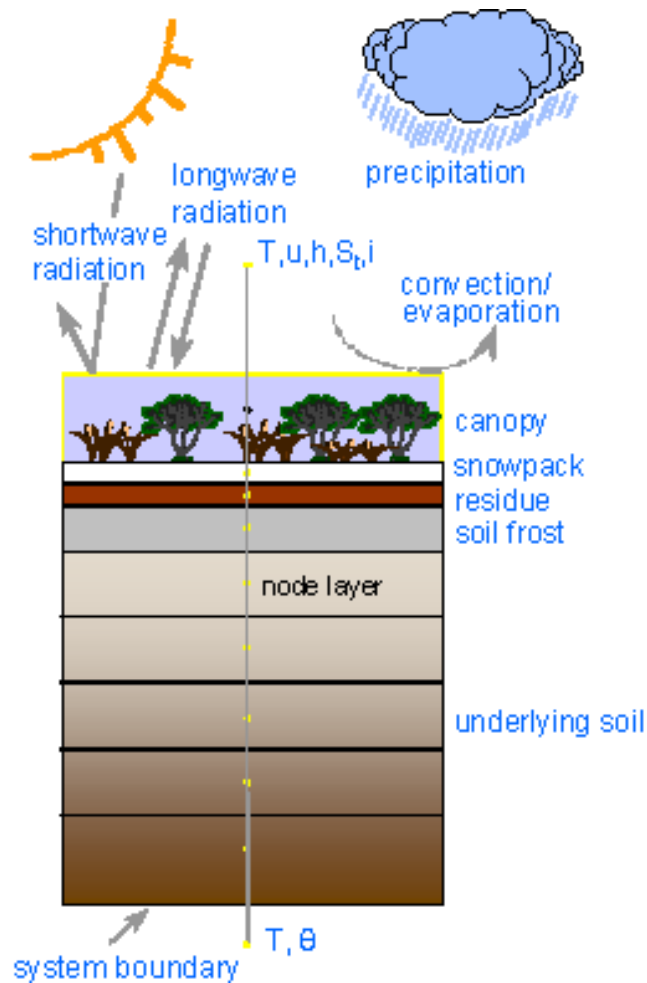# The Simultaneous Heat and Water (SHAW) Model: Technical Documentation

Version 3.0

Gerald N. Flerchinger
Northwest Watershed Research Center
USDA Agricultural Research Service
Boise, Idaho

Table of Contents

The SHAW Model

The Simultaneous Heat and Water (SHAW) model, originally developed to simulate soil freezing and thawing (Flerchinger and Saxton, 1989), simulates heat, water and solute transfer within a one-dimensional profile which includes the effects of plant cover, dead plant residue, and snow. The model's ability to simulate heat and water movement through plant cover, snow, residue and soil for predicting climate and management effects on soil freezing, snowmelt, runoff, soil temperature, water, evaporation, and transpiration has been demonstrated. Unique features of the model include: simultaneous solution of heat, water and solute fluxes; detailed provisions for soil freezing and thawing; and a sophisticated approach to simulating transpiration and water vapor transfer within a multi-species plant canopy. Information from the model can be used to assess management and climate effects on biological and hydrological processes, including seedling germination, plant establishment, insect populations, soil freezing, infiltration, runoff, and ground-water seepage.

The physical system described by the SHAW model consists of a vertical, one-dimensional profile extending from the vegetation canopy, snow, residue, or soil surface to a specified depth within the soil (Figure 1). The system is represented by integrating detailed physics of a plant canopy, snow, residue and soil into one simultaneous solution.

Daily or hourly weather conditions of air temperature, wind speed, humidity, solar radiation, and precipitation above the upper boundary and soil conditions at the lower boundary are used to define heat and water fluxes into the system. A layered system is established through the plant canopy, snow, residue and soil and each layer is represented by an individual node. Energy, moisture and solute fluxes are computed between nodes for each time step, and balance equations for each node are written in implicit finite-difference form.

After solving the energy, water and solute balance for the time step, adjustments are made for precipitation, snowmelt, settling of the snowpack, interception, and infiltration at the end of each time step. The model then optionally outputs a summary of the water balance, surface energy transfer, snow depth, and frost depth as well as temperature, moisture, and solute profiles.
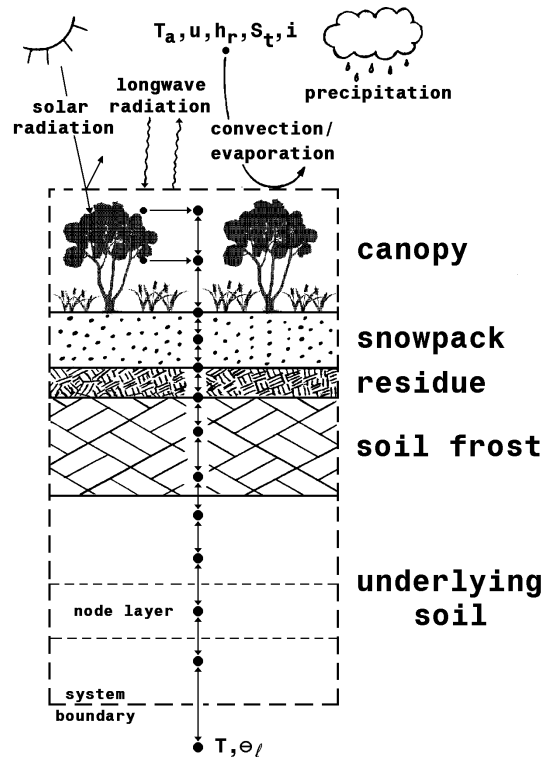

Figure 1: Physical system described by the SHAW model. T_a is temperature, u is windspeed, h_r is relative humidity, S_t is solar radiation, i is precipitation, T is soil temperature, and θ_l is soil water content.

The following sections describe in detail each major component of the SHAW model. These include radiation and convective transfer at the surface boundary, energy and moisture balance of the plant, snow, residue and soil layers, solute transport in the soil, and precipitation-infiltration processes.

Surface Energy and Water Fluxes

The interrelated energy and water fluxes at the surface boundary are computed from weather observations of air temperature, wind speed, relative humidity and solar radiation. The surface energy balance may be written as

$$R_n + H + L_v E + G = 0 \qquad\qquad [1]$$

where R_n is net all-wave radiation (W m^{-2}), H is sensible heat flux (W m^{-2}), L_vE is latent heat flux (W m^{-2}), G is soil or ground heat flux (W m^{-2}), L_v is latent heat of evaporation (J kg^{-1}), and E is total evapotranspiration from the soil surface and plant canopy (kg m^{-2} s^{-1}).

Net Radiation

Net radiation consists of absorbed solar radiation, absorbed long-wave radiation, and emitted long-wave radiation. From incoming atmospheric solar and long-wave radiation, a full radiation balance is computed for each layer within the plant canopy, residue and surface (snow or soil) by computing the reflection, transmission, scattering and absorption of each layer. Net solar radiation at the snow surface is distributed through the snow based on extinction coefficient.

Atmospheric incoming radiation to the surface

Solar radiation absorbed within the system is computed from the observed total incoming solar radiation (S_t). Incoming long-wave radiation to the system is estimated by the model based on cloud cover, which in turn is estimated from S_t.

Total incoming solar radiation (S_t) consists of direct (or beam, S_b), and diffuse (S_d) components. Because direct and diffuse are absorbed and transmitted differently, total solar radiation is separated in to the two components by the following equation developed by Bristow et al. (1985):

$$\tau_d = \tau_t \left[1 - \exp\left(\frac{0.6\,(1 - \tau_{t,\max} / \tau_t)}{\tau_{t,\max} - 0.4} \right) \right] \qquad\qquad [2]$$

where τ_d is the atmospheric diffuse transmission coefficient ($S_d / S_{b,o}$), τ_t is the atmospheric total transmission coefficient ($S_t / S_{b,o}$), $\tau_{t,\max}$ is the maximum clear-sky tranmissivity of the atmosphere (taken as 0.76), and $S_{b,o}$ is total solar radiation incident on a horizontal surface at the outer edge of the atmosphere (W m^{-2}). Hourly values for $S_{b,o}$ are calculated from the solar constant, S_o (~1360 W m^{-2}), and the sun's altititude above the horizon, ϕ_s. Direct solar radiation incident on a sloping surface is related to that on a horizontal surface by

$$S_s = S_b \sin\beta / \sin\phi_s \qquad\qquad [3]$$

where β is the angle which the sun's rays make with the sloping surface and ϕ_s is computed based on the latitude of the site, the time of year, and the hour of the day. Long-wave radiation emitted by an object follows the Stefan-Boltzman equation, presented as:

$$L_o = \varepsilon\sigma T_K^4 \qquad\qquad [4]$$

where ε is emissivity, σ is the Stefan-Boltzman constant (5.6697×10^{-8} W m^{-2} K^{-4}), and T_K is temperature of the object (K). Flerchinger et al. (2009a) compared numerous approaches for estimating long-wave radiation from clear and cloudy skies. They selected the approach given by Dilley and Obrien (1998) for estimating down-welling clear-sky long-wave radiation:

$$L_{clr} = 59.38 + 113.7\left(\frac{T_o}{273.16}\right)^6 + 96.96\sqrt{w/2.5} \qquad\qquad [5]$$

Long-wave radiation for cloudy skies is obtained by back-calculating clear-sky emissivity, ε_{clr}, from L_{clr} and Eqn. [4] above, then adjusting the emissivity for the fraction of cloud cover from (Campbell, 1985)

$$\varepsilon_{ac} = (1 - 0.84C_c)\varepsilon_{clr} + 0.84C_c \qquad\qquad [6]$$

where ε_{ac} is the atmospheric emissivity adjusted for cloud cover. Fraction of cloud cover, C_c, is assumed constant for the day and is estimated from (Flerchinger et al., 2009a)

$$C_c = 1.333 - 1.666\tau_t . \qquad\qquad [7]$$

Here τ_t, the atmospheric transmissivity, is the ratio of measured solar radiation, S_t, to that incident on the outer edge of the atmosphere ($S_{b,o}$). Assumptions inherent in this expression are complete cloud cover for $\tau_t < 0.20$ and clear skies for $\tau_t > 0.80$. Emitted long-wave radiation for each material, L_o, is computed from the Stefan-Boltzman Law using a surface temperature computed from a detailed energy balance for the system profile.

The net radiation absorbed for each layer depends not only on the incoming radiation from above, but on the reflected, scattered and emitted radiation from other layers within the plant canopy, snow, residue, soil system. Therefore a radiation balance similar to that described by Norman (1979) and Bristow et al. (1986) is performed by computing the direct, and upward and downward diffuse radiation fluxes above and below each layer. Transmission and reflectance within each layer is described in the following subsections.

Solar radiation within the canopy
Several modifications for radiation transfer were introduced into version 3.0 of the SHAW model. These included: a more generalized expression for canopy transmissivity to short-wave radiation and long-wave radiation; directional scattering of radiation; inclusion of effects of short-wave radiation transmission through the plant leaves; and long-wave fluxes based on leaf temperature rather than canopy air temperature. These modification are described in Flerchinger et al. (2007, 2009b). Solar and long-wave radiation exchange between canopy layers, residue layers and the snow or soil surface are computed by considering direct, and upward and downward diffuse radiation being transmitted, reflected and absorbed.

Upward flux of diffuse short-wave radiation above canopy layer i (numbered from the top of the canopy) is computed as

$$S_{u,i} = \left[\tau_{d,i} + (\alpha_{l,d,i}f_{d,i,\downarrow\downarrow} + \tau_{l,d,i}f_{d,i,\downarrow\uparrow})(1-\tau_{d,i})\right]S_{u,i+1}$$
$$+ (\alpha_{l,d,i}f_{d,i,\downarrow\uparrow} + \tau_{l,d,i}f_{d,i,\downarrow\downarrow})(1-\tau_{d,i})S_{d,i} \qquad [8]$$
$$+ (\alpha_{l,b,i}f_{b,i,\downarrow\uparrow} + \tau_{l,b,i}f_{b,i,\downarrow\downarrow})(1-\tau_{b,i})S_{b,i}$$

where $\tau_{d,i}$ is the transmissivity of canopy layer i to diffuse radiation, $\tau_{b,i}$ is the transmissivity of canopy layer i to direct (or beam) radiation, $\alpha_{l,b,i}$ and $\tau_{l,b,i}$ are the effective albedo and leaf transmittance of canopy layer i to direct radiation, $\alpha_{l,d,i}$ and $\tau_{l,d,i}$ are the effective albedo and leaf transmission to diffuse radiation within canopy layer i, $f_{b,i,\downarrow\uparrow}$ and $f_{d,i,\downarrow\uparrow}$ are the fractions of reflected direct and diffuse radiation scattered backward (e.g. downward radiation scattered upward), and $f_{b,i,\downarrow\downarrow}$ and $f_{d,i,\downarrow\downarrow}$ are the fractions of reflected direct and diffuse radiation scattered forward, and $S_{d,i}$ and $S_{b,i}$ are downward diffuse and direct radiation entering canopy layer i. A similar expression can be written for downward radiation at any point in the canopy. Flerchinger and Yu (2007) developed expressions for the fractions of forward and back scattered direct and diffuse radiation. It should be noted that the fraction of radiation transmitted through the leaves and scattered forward is equal to that reflected and scattered backward. Downward direct radiation anywhere within the canopy can be computed explicitly knowing the direct radiation from the atmosphere and the transmissivity of each canopy layer.

The SHAW model will simulate a multi-species canopy, and the transmissivity to direct radiation for each canopy layer is calculated from:

$$\tau_{b,i} = \exp\left(\sum_{j=1}^{NP}\Omega_j K_{b,j}L_{AI,i,j}\right) \qquad [9]$$

where $L_{AI,i,j}$ and $K_{b,j}$ are leaf area index and extinction coefficient for direct radiation respectively for plant species j and canopy layer i, Ω_j is a clumping factor to account for the fact that leaves are less efficient at intercepting radiation when clumped together (Campbell and Norman, 1998), and NP is the number of plant species. The extinction coefficient is dependent on the direction of the radiation source and the orientation of the plant leaves. Campbell and Norman (1998) present an expression for $K_{b,j}$ assuming an ellipsoidal leaf orientation:

$$K_{b,j} = \frac{\sqrt{x^2 + \tan^2\phi}}{x + 1.774(x+1.182)^{-0.733}} \qquad [10]$$

where x is a coefficient relating to leaf orientation and ϕ is the zenith angle of the radiation. The value of x is related to the vertical (a) and horizontal (b) axes of the ellipsoid by $x=b/a$. For vertically-oriented leaf elements, $x = 0$; for randomly-distributed or spherically-oriented elements, $x = 1$; and for horizontal elements, $x = \infty$, (although $x = 5$ approximates infinity). Typical values of x for different crops are given by Campbell and Norman (1998).

The transmission of diffuse radiation from a given direction is identical to that for direct radiation for that direction. Thus, the transmission of diffuse radiation through the canopy can be calculated by integrating the expression for direct radiation over all directions within the hemisphere (Campbell and Norman, 1998):

$$\tau_{d,i} = 2\int_0^{\pi/2}\tau_{b,i}(\phi)\sin\phi\cos\phi\,d\phi . \qquad [11]$$

where $\tau_{d,i}$ is the fraction of diffuse radiation passing through a canopy layer unimpeded by vegetation. This expression requires numerical integration, however Flerchinger and Yu (2007) developed a very close approximation for the diffuse radiation extinction coefficient:

$$K_{d,j} = \frac{K_{d\infty} L_{AI,j}{}^{A} + B}{L_{AI,j}{}^{A} + B}$$
[12]

where $L_{AI,j}$ is total leaf area index for plant j, A and B are empirical coefficients, and $K_{d\infty}$ is the asymptote that $K_{d,j}$ approaches at infinite L_{AI} for a given value of x. Flerchinger and Yu (2007) developed the following approximate relation for $K_{d\infty}$:

$$K_{d\infty} = \begin{cases} \dfrac{2}{\pi} \arctan(x) & x \le 1.0 \\[2mm] \dfrac{x^{C}}{x^{C} + 1.0} & x > 1.0 \end{cases}$$
[13]

where C is an empirical coefficient. Suggested values for A, B and C are 0.65, 1.9, and 1.46, respectively. Flerchinger et al. (2009b) demonstrated that total leaf area index for plant type, j, ($L_{AI,j}$) should be used to compute $K_{d,j}$ rather than using the leaf area for each individual layer. Flerchinger and Yu (2007) also presented relations for direct and diffuse scattered radiation, $f_{d,i,\downarrow\uparrow}$ and $f_{d,i,\downarrow\downarrow}$.

In a canopy layer with multiple plant types, the effective transmissivity, albedo, and scattering functions must be weighted by each plant type within the layer. Effective albedo for diffuse radiation of canopy layer i is calculated as a weighted average of the layer tranmissivity for each plant type by the expression

$$\alpha_{l,d,i} = \frac{\sum_{j=1}^{NP} \alpha_{l,j}(1 - \tau_{d,i,j})}{\sum_{j=1}^{NP}(1 - \tau_{d,i,j})}$$
[14]

where $\alpha_{l,j}$ is the albedo of plant species j, and $\tau_{d,i,j}$ is the diffuse transmissivity of canopy layer i based on leaf area of plant species j. A similar expression can be written for $\tau_{l,d,i}$. Because the layer transmissivity is different for direct and diffuse radiation, the effective albedo and leaf transmission of the layer may be different for direct and diffuse radiation. The scattering functions must also be weighted differently for direct and diffuse radiation. For direct radiation, the effective fraction of backward scattered radiation is

$$f_{b,i,\downarrow\uparrow} = \frac{\sum_{j=1}^{NP} f_{b,j,\downarrow\uparrow} \alpha_{l,j}(1 - \tau_{i,j})}{\sum_{j=1}^{NP} \alpha_{l,j}(1 - \tau_{i,j})}$$
[15]

where $f_{b,j,\downarrow\uparrow}$ is the fraction of reflected direct radiation scattered backward for plant j. A similar expression can be written for the scattered direct radiation transmitted through the leaves and scattered diffuse reflected and transmitted radiation. Although the fraction of radiation transmitted through the leaves and scattered forward is equal to that reflected and scattered backward for a given leaf, this is not necessarily true for the entire canopy layer if the plants within the layer have differing leaf albedos or leaf transmissivities.

A similar expression to that for $S_{u,i}$ presented above can be written for downward diffuse

radiation. This creates a set of 2(N+1) equations where multiple scatterings are implicitly included and the boundary condition $S_{d,1}$ is the incoming diffuse radiation from the atmosphere and $S_{u,N+1}$ is the solar radiation reflected by the soil or residue layer:

$$S_{u,N+1} = (1-\alpha_s)(S_{d,N+1} + S_{b,N+1})$$ [16]

where α_s is the albedo of the residue or soil surface. The system of equations is linear and can be solved directly, similar to the approach described by Zhao and Qualls (2005). Net short-wave radiation absorbed by plant type j within canopy layer i is computed from

$$S_{n,i,j} = \frac{(1-\alpha_{l,j}-\tau_{l,j})(1-\tau_{d,i,j})}{\sum\limits_{j=1}^{NP}(1-\alpha_{l,j}-\tau_{l,j})(1-\tau_{d,i,j})}(1-\tau_{d,i})\left(S_{d,i}+S_{u,i+1}\right)$$

$$+\frac{(1-\alpha_{l,j}-\tau_{l,j})(1-\tau_{b,i,j})}{\sum\limits_{j=1}^{NP}(1-\alpha_{l,j}-\tau_{l,j})(1-\tau_{b,i,j})}(1-\tau_{b,i})S_{b,i}$$ [17]

where $\tau_{d,i,j}$ and $\tau_{b,i,j}$ are the computed diffuse and direct transmissivities for plant j and of canopy layer i based on its leaf area and respective extinction coefficients, and $\alpha_{l,j}$ and $\tau_{l,j}$ are the leaf reflectance and transmission of plant j.

Solar radiation within the residue

Transmission, absorption and scattering of direct radiation within the residue is computed similar to that for plant canopy and is computed as part of the solution matrix for the canopy if a plant canopy is present. The transmission of direct radiation for the residue present is calculated from

$$\tau_{b,r} = (1-F_r)\sin\beta = \exp(K_{b,r}W_r)\sin\beta$$ [18]

where F_r is the fraction of surface area covered by the residue layer ($m^2\,m^{-2}$), $K_{b,r}$ is the extinction coefficient for direct radiation through the residue, W_r is the dry mass of residue on the surface, and β is the angle which the sun's rays make with the surface. Transmission to diffuse radiation within the residue layer is computed as

$$\tau_{d,r} = 0.667(1-F_r) = 0.667\exp(K_{b,r}W_r) \quad .$$ [19]

However, the residue can be divided into several individual layers. Transmission of direct and diffuse radiation through each individual layer is computed by back-calculating the extinction coefficient, $K_{b,r}$, from the input F_r and W_r. Radiation reflected and scattered by each residue layer may be absorbed by adjacent canopy layers, residue layers and the soil surface, or lost to the atmosphere. No solar or long-wave radiation is considered within the residue layer if it snow-covered.

Solar radiation at the snow surface

Albedo of the snow for diffuse radiation is computed from (Anderson, 1976):

$$\alpha_{sp} = 1 - 0.206\,C_v\,d_s^{1/2}$$ [20]

where C_v is an empirical coefficient used to calculate the extinction coefficient and d_s is grain-size diameter of ice crystals (mm). Grain-size is calculated from (Anderson, 1976):

$$d_s = G_1 + G_2(\rho_{sp}/\rho_l)^2 + G_3(\rho_{sp}/\rho_l)^4$$ [21]

where G_1, G_2 and G_3 are empirical coefficients, ρ_{sp} is density of the snow at the surface and ρ_l is density of liquid water. Albedo of shallow snowpacks (less than 4 cm) is adjusted based on the

albedo of the underlying material.

Reflection of direct radiation differs with the visible and near-infrared spectrums and is influenced by sun angle.   Albedo for the visible and near-infrared fractions are given by

$$\alpha_{sp,v} = 0.001375(1000d_s)^{1/2}(1-\sin\beta)\alpha_{sp} \tag{22}$$

and

$$\alpha_{sp,ir} = 0.002(1000d_s)^{1/2}(1-\sin\beta)\alpha_{sp} \tag{23}$$

An effective albedo for direct radiation is computed from a weighted average of the visible and near-infrared albedos, assuming 58% of the total solar radiation is in the visible spectrum.   Net solar radiation at the snow surface is distributed through multiple layers of the snow based on solar radiation extinction through the snowpack, as given subsequently in Eqns. [52] to [53].

Solar radiation at the soil surface

Soil albedo varies with soil water content and is calculated from (Idso et al., 1975)

$$\alpha_s = \alpha_d \exp(-a_\alpha \theta_l) \tag{24}$$

where α_d is albedo of dry soil, θ_l is surface volumetric water content and a_α is an empirical coefficient.

Long-wave radiation

The expression for upward long-wave radiation through the canopy and residue is similar to that for short-wave radiation, except that leaf transmittance of long-wave radiation can be ignored and long-wave emittance replaces the term for direct short-wave radiation:

$$L_{u,i} = \left[\tau_{d,i} + (1-\varepsilon_c)f_{d,i,\downarrow\downarrow}(1-\tau_{d,i})\right]L_{u,i+1}$$

$$+ (1-\varepsilon_c)f_{d,i,\downarrow\uparrow}(1-\tau_{d,i})L_{d,i} + \frac{1-\tau_{d,i}}{\sum_{j=1}^{NP}(1-\tau_{d,i,j})}\sum_{j=1}^{NP}(1-\tau_{d,i,j})\varepsilon_c\sigma T_{l,i,j}^4. \tag{25}$$

Here the emissivity of the canopy elements, ε_c, is assigned to all plant types, and $T_{l,i,j}$ is the leaf temperature of plant j in canopy layer i. As with the short-wave radiation, this creates a set of $2(N+1)$ set of equations where the boundary condition $L_{d,1}$ is the incoming atmospheric long-wave radiation and $L_{u,N+1}$ is the long-wave radiation reflected and emitted by the soil or residue layer:

$$L_{u,N+1} = (1-\varepsilon_s)L_{d,N+1} + \varepsilon_s\sigma T_s^4 \tag{26}$$

where ε_s is the surface emissivity (snow or soil).   Net long-wave radiation absorbed by each plant type within the canopy layer is computed from

$$L_{n,i,j} = \varepsilon_c(1-\tau_{d,i})\frac{1-\tau_{d,i,j}}{\sum_{j=1}^{NP}(1-\tau_{d,i,j})}\left(L_{d,i} + L_{u,i+1} - \sigma T_{l,i,j}^4\right). \tag{27}$$

As with solar radiation, no long-wave radiation transfer is assumed through the residue when it is snow-covered; alternatively, the thermal conductivity of the snow is used for heat transfer through the residue voids.

Sensible and Latent Heat Fluxes

Sensible and latent heat flux components of the surface energy balance are computed from temperature and vapor gradients between the canopy-residue-soil surface and the atmosphere.

Sensible heat flux is calculated from (Campbell, 1977):

$$H = -\rho_a c_a \frac{(T - T_a)}{r_H} \tag{28}$$

where ρ_a, c_a and T_a are the density (kg m^{-3}), specific heat (J kg^{-1} C^{-1}) and temperature (C) of air at the measurement reference height z_{ref}, T is the temperature (C) of the exchange surface, and r_H is the resistance to surface heat transfer (s m^{-1}) corrected for atmospheric stability. Here, the exchange surface is either the top of the canopy, the residue layer, the snow surface or the soil surface depending on the system profile. Latent heat flux is associated with transfer of water vapor from the exchange surface to the atmosphere, which is given by

$$E = \frac{(\rho_{vs} - \rho_{va})}{r_v} \tag{29}$$

where ρ_{vs} and ρ_{va} are vapor density (kg m^{-3}) of the exchange surface and at the reference height z_{ref}, and the resistance value for vapor transfer, r_v, is taken to be equal to r_H. The resistance to convective heat transfer, r_H, is computed from

$$r_H = \frac{1}{u_* k} \left[\ln\left(\frac{z_{ref} - d + z_H}{z_H} \right) + \psi_H \right] \tag{30}$$

where u_* is the friction velocity (m s^{-1}) computed from

$$u_* = u k \left[\ln\left(\frac{z_{ref} - d + z_m}{z_m} \right) + \psi_m \right]^{-1}, \tag{31}$$

k is von Karman's constant, d is the zero plane displacement, u is windspeed, z_H and z_m are the surface roughness parameters for the temperature and momentum profiles, and ψ_H and ψ_m are diabatic correction factors for heat and momentum, computed as a function of atmospheric stability. Atmospheric stability is calculated as a ratio of thermally induced to mechanically induced turbulence (Campbell, 1977):

$$s = \frac{k z_{ref} g H}{\rho_a c_a T_K u_*^3} \tag{32}$$

where g is gravitational acceleration. Under stable conditions ($s > 0$),

$$\psi_H = \psi_m = 4.7s.$$

For unstable conditions, ($s < 0$), ψ_m is approximately 0.6 ψ_H (Norman, 1979) and

$$\psi_H = -2 \ln\left(\frac{1 + \sqrt{1 - 16s}}{2} \right). \tag{33}$$

When there is no canopy present, the user-supplied value for z_m is used and d is set to zero. Surface roughness parameter for the temperature profile, z_H is assumed to be 0.2 z_m. For full plant canopy, the surface roughness parameter for the momentum profile, z_m, is taken as 0.13 times the plant canopy height and the zero plane displacement, d, is 0.77 times canopy height. Version 3.0 of the SHAW model includes provisions for a sparse canopy (Flerchinger et al., 2012). Thus, the

following estimation of the effective zero-plane displacement, d_e, for sparse canopies was adopted from Zeng and Wang (2007):

$$d_e = Vd + (1 - V)d_g \quad .$$

[34]

Here, d is the zero plane displacement assumed for full canopy closure, and d_g and z_{mg} are the displacement height and surface roughness beneath the plant canopy; z_{mg} is input to the model while d_g is set equal to snow depth or taken as zero for a residue or soil surface. V is a function of leaf area index:

$$V_e = \frac{1 - \exp[- \min(L_{AI}, L_{cr})]}{1 - \exp(-L_{cr})} \quad\quad\quad\quad [35]$$

where L_{AI} is total leaf area index of all plants, and L_{cr} is a critical value assumed for full canopy cover, taken as 2.0. Based on wind profile analyses, Flerchinger et al. (2012) adopted the following linear interpolation for roughness z_{me} in lieu of the logarithmic interpolation used by Zeng and Wang (2007):

$$z_{me} = Vz_m + (1 - V)z_{mg} \quad . \quad\quad\quad\quad [36]$$

To account for a sparse canopy over a relatively dense understory, the above algorithms for Eqns. [34]**Error! Reference source not found.** and [35] were modified such that the leaf area index of any plant type shorter than d_e computed for the taller plants was not included in total leaf area index. The effective canopy height, h_{ce}, was computed based on the relation often taken for d of full canopies: $d_e = 0.77h_{ce}$. Thereby, the transfer coefficients through very sparse canopies approach that for no canopy as L_{AI} and h_{ce} approach zero.

Ground Heat Flux

The net radiation and turbulent heat fluxes in Eqn. [1] interface with ground heat flux, G, through the surface temperature of the canopy, residue or soil. This surface temperature must satisfy the solution of the heat flux equations for the entire canopy/residue/soil profile, which is solved simultaneously and iteratively with the surface energy balance. Details of heat and water flux equations for the plant canopy, snow, residue and soil are described in the following sections.

Energy Fluxes Within the System

Heat Flux Through the Canopy

Heat and vapor fluxes within the canopy are determined by computing transfer between layers of the canopy and considering the source terms for heat and transpiration from the canopy leaves for each layer within the canopy. Modifications for turbulent transfer through the canopy introduced into version 3.0 of the SHAW model are described by Flerchinger et al. (2012, 2015), which include far-field Lagrangian theory for turbulent transfer and stability corrections. Heat flux and temperature within the air space of the canopy are described by

$$\rho_a c_a \frac{\partial T}{\partial t} = \frac{\partial}{\partial z}\left(\rho_a c_a k_e \frac{\partial T}{\partial z}\right) + H_l \qquad [37]$$

where the terms (W m^{-3}) represent: energy storage within the canopy air space; net heat transfer into a layer within a canopy; and a heat source term for heat transfer from the canopy elements (leaves) to the air space within the canopy. In this equation, ρ_a, c_a and T are density (kg m^{-3}), specific heat capacity (J kg^{-1} C^{-1}) and temperature (C) of the air within the canopy, t is time (s), z is height from the top of the canopy (m), k_e is a transfer coefficient within the canopy (m^2 s^{-1}), and H_l is heat transferred from the vegetation elements (leaves) to the air space within the canopy (W m^{-3}).

Transfer within the canopy

Within-canopy turbulence is computed using Lagrangian far field dispersion (Raupach, 1989) with the atmospheric stability corrections given by Leuning (2000). The Lagrangian far field dispersion coefficient (m^2 s^{-1}) with stability corrections is given by

$$K_f = \sigma_w^2 \tau_L / \varphi_h \varphi_w \qquad [38]$$

where σ_w is the standard deviation of the vertical velocity, τ_L is the Lagrangian time scale, and φ_h and φ_w are the stability functions. Leuning (2000) presented equations to ensure a smooth transition for σ_w and τ_L above and through the canopy. Instead of the approximation for σ_w used by Flerchinger et al. (2012) which underestimated σ_w deep within the canopy, the following expression provided by Leuning (2000) is used:

$$\sigma_w = 0.2\exp\left(\frac{1.5z}{h_{ce}}\right)u_*\varphi_w, \quad z/h_{ce} \le 0.8 \qquad [39]$$

where z is height within the canopy. For values of $z/h_{ce} > 0.8$, σ_w is linearly interpolated between values of 0.664, 1.1, and 1.25 at z/h_{ce} values of 0.8, 1.5 and 2.3, respectively, to provide a close approximation to the non-rectangular hyperbola proposed by Leuning (2000). The Lagrangian time scale is approximated by

$$\tau_L = \begin{cases} 0.4h_{ce}/(u_*\varphi_H\varphi_w^2), & 0.25 \le z/h_{ce} \le 2.3 \\ 1.6z/(u_{g*}\varphi_H\varphi_w^2), & z/h_{ce} < 0.25 \end{cases} \qquad [40]$$

For $z/h_{ce} > 2.3$, K_f is computed directly from

$$K_f = k(z - d_e)u_*/\varphi_H, \quad z/h_{ce} > 2.3 . \qquad [41]$$

Clearly this condition will occur within the canopy only for very sparse canopies ($L_{AI} < 0.47$). Stability within the canopy is based on the gradient Richardson number; expressions for the stability functions φ_H and φ_w are given by Flerchinger et al. (2012) and are the same as used by Leuning (2000). The turbulent transfer coefficient across each canopy layer is integrated by computing τ_L and σ_w at the top and bottom of each canopy layer and at any of the breaks in the functions for σ_w and τ_L (i.e. $z/h_{ce} = 0.25$, 0.8, 1.5 and 2.3) contained within the layer.

The stability functions φ_h and φ_w are limited to the range of -2 to 1 and are computed as

$$\varphi_w = \begin{cases} (1 - 3\zeta), & -2 \le \zeta \le 0 \\ (1 + 0.2\zeta), & 0 \le \zeta \le 1 \end{cases} \qquad [42]$$

and

$$\varphi_h = \begin{cases} (1-16\zeta)^{-1/2}, -2 \le \zeta \le 0 \\ (1+5\zeta) \quad\quad, \quad 0 \le \zeta \le 1 \end{cases} \tag{43}$$

The gradient Richardson number is used within the canopy:

$$R_i = \frac{g(T_i - T_g)z_i}{(T_i + 273.16)^2(u_{c,i} - u_g)^2} \tag{44}$$

Here T_i, $u_{c,i}$, and z_i, are temperature wind speed and height of canopy layer i, and u_g is wind speed at the ground surface. Leuning (2000) used the relation between ζ and R_i presented by Kaimal and Finnigan (1994):

$$\zeta = \begin{cases} R_i, \quad\quad\quad\quad -2 \le \zeta \le 0 \\ R_i/(1-5R_i), \quad 0 \le \zeta \le 0.175 \end{cases} \tag{45}$$

The value of R_i is limited to 0.175 to minimize the high sensitivity of ζ on R_i as R_i approaches 0.2.

Heat transfer from the canopy elements

Heat transfer from the vegetation elements (leaves) to the air space within a canopy layer for a given plant species (W m^{-2}) is computed from:

$$H_{l,i,j} = -2\rho_a c_a L_{i,j} \frac{(T_{l,i,j} - T_i)}{r_{h,i,j}}. \tag{46}$$

Here, $L_{AI,i,j}$, and $T_{l,i,j}$, are one-sided leaf area index and leaf temperature of plant species j within canopy layer i, T_i is air temperature within canopy layer i, and resistance to convective transfer from the canopy leaves per unit leaf area index, $r_{h,i,j}$ (s m^{-1}), is computed from Campbell and Norman, 1998:

$$r_{h,i,j} = 7.4\rho_a \sqrt{\frac{d_l}{u_{c,i}}} = \frac{7.4P}{R(T_i + 273.16)}\sqrt{\frac{d_{l,j}}{u_{c,i}}} \tag{47}$$

where $r_{h,i,j}$ is the resistance to heat (s/m) from the leaves in canopy layer i for plant type j, P is atmospheric pressure (Pa), $d_{l,j}$ is the characteristic dimension of the leaves for plant species j, and $u_{c,i}$ is windspeed in canopy layer i based on an exponential decay computed from cumulative leaf area index (Nikolov and Zeller, 2003).

Leaf temperature for each layer within the canopy ($T_{l,i,j}$) is determined from a leaf energy balance of the canopy layer:

$$S_{n,i,j} + L_{n,i,j} + H_{l,i,j} + L_v E_{l,i,j} = m_{c,i,j} c_c \frac{\partial T_{l,i,j}}{\partial t}. \tag{48}$$

Here, $S_{n,i,j}$ and $L_{n,i,j}$ are net short-wave and long-wave radiation (W m^{-2}) for the leaf surfaces within canopy layer i for plant species j, L_v is the latent heat of vaporization, and $E_{l,i,j}$ is vapor flux (kg s^{-1} m^{-2}) from the leaf surfaces, $m_{c,i,j}$ is the biomass of plant j within canopy layer i, and c_c is the heat capacity of the biomass. Water uptake, transpiration and leaf temperature are coupled through the energy balance of the leaf, which is calculated for each plant species within each canopy layer. The leaf energy balance is computed iteratively with heat and water vapor transfer equations (Eqns. 24 and 46) and transpiration within the canopy (Eqns. 47 and 49).

Heat Flux within the Snow

The energy balance for each layer within the snowpack is written as follows:

$$\rho_{sp} c_i \frac{\partial T}{\partial t} + \rho_l L_f \frac{\partial w_{sp}}{\partial t} = \frac{\partial}{\partial z}\left[k_{sp} \frac{\partial T}{\partial z} \right] + \frac{\partial R_n}{\partial z} - L_s \left(\frac{\partial q_v}{\partial z} + \frac{\partial \rho_v}{\partial t} \right) \qquad [49]$$

where the terms (W m^{-3}) represent, respectively: specific heat term for change in energy stored due to a temperature increase; latent heat required to melt snow; net thermal conduction into a layer; net radiation absorbed with a layer; and net latent heat of sublimation. Heat transferred by liquid movement in the snowpack is not considered in the energy balance equation; at the end of each time step a mass balance of the snowpack is computed to adjust the snowpack for melt, water percolation, and thermal advection. Symbols in the above equation are as follows: ρ_{sp}, w_{sp}, and k_{sp} are density (kg m^{-3}), volumetric liquid water content (m^3 m^{-3}), and thermal conductivity and the snow (W m^{-1} C^{-1}); c_i is specific heat capacity of ice (J kg^{-1} C^{-1}); ρ_l is density of water (kg m^{-3}); R_n is net downward radiation flux within the snow (W m^{-2}); L_f and L_s are latent heat of fusion and sublimation (J kg^{-1}); q_v is vapor flux (kg s^{-1} m^{-2}); and ρ_v is vapor density (kg m^{-3}) within the snow.

Specific heat

At temperatures below 0 °C, net energy absorbed by the snow results in a change in temperature. The volumetric specific heat of snow is computed from the density of the snow, ρ_{sp} and the specific heat of ice, which is a function of temperature (Anderson, 1976):

$$c_i = 92.96 + 7.37 T_K \qquad [50]$$

where T_K is temperature of the snow in Kelvin.

Latent heat of fusion

At 0 °C, the net energy absorbed by the snowpack results in melting of ice. Ice content of the snowpack is assumed constant over the hour time-step and is adjusted for any melt at the end of the time step.

Thermal conduction

The primary mechanism for energy transfer within a snowpack is thermal conduction between and within ice crystals. Thermal conductivity of snow has been empirically related to density by many researchers, although geometry of the snow crystals is important as well. An expression of the form

$$k_{sp} = a_{sp} + b_{sp} (\rho_{sp} / \rho_l)^{c_{sp}} \qquad [51]$$

is suggested by Anderson (1976) and will fit many empirically derived correlations. Here a_{sp}, b_{sp}, and c_{sp}, are empirical coefficients; Anderson (1976) suggests values of 0.021 W m^{-1} C^{-1}, 2.51 W m^{-1} C^{-1} and 2.0, respectively.

Radiation absorption

Because snow is translucent, solar radiation entering the surface of the snowpack is attenuated and absorbed throughout the snowpack. The net solar radiation flux at a depth z can be expressed as

$$S_z = (S_s + S_d)(1 - \alpha_{sp}) \ e^{-vz}. \qquad [52]$$

where ($S_s + S_d$) is the total solar radiation incident on the snow surface. The extinction coefficient,

v, for radiation penetration through the snow is calculated from (Anderson, 1976)

$$v = 100 C_v (\rho_{sp} / \rho_l) d_s^{-1/2} \tag{53}$$

where C_v is taken as 1.77 mm$^{1/2}$ cm^{-1} (Flerchinger et al., 1996a) and d_s is grain-size diameter of ice crystals (mm; Eqn. [21]).

Latent heat of sublimation

Latent heat transfer by sublimation is a result of vapor transfer through the snowpack in response to temperature gradients. Vapor density in snow is assumed equal to the saturated vapor density over ice, and therefore is solely a function of temperature. Warmer parts of the snowpack have a higher vapor density; vapor will therefore diffuse toward cooler parts, where, due to over-saturation, sublimation will occur and latent heat is released. Vapor flux through the snowpack is calculated by

$$q_v = D_e \frac{\partial \rho_v}{\partial z} \tag{54}$$

where D_e is the effective diffusion coefficient (m s^{-2}) for water vapor in snow, and ρ_v is the temperature-dependent vapor density within the snow. The net latent heat of sublimation for a layer in the snowpack is equal to the increase in vapor density minus the net transfer of vapor to that layer.

Heat Transport Processes in the Residue

The energy balance for a layer of plant residue is expressed as

$$C_r \frac{\partial T}{\partial t} = \frac{\partial}{\partial z} \left(k_r \frac{\partial T}{\partial z} \right) - L_v \frac{\partial}{\partial z} \left(\frac{(h_r \rho_{vs}' - \rho_v)}{r_h} \right) + \frac{\partial R_n}{\partial z} \tag{55}$$

where the terms (W m^{-3}) represent, respectively: specific heat term for change in energy stored due to a temperature increase; net thermal convection/conduction into a layer; net latent heat of evaporation from residue elements; and net absorption of radiant heat. Symbols here are defined as follows: C_r and T are volumetric heat capacity (J m^{-3} C^{-1}) and temperature (C) of residue; k_r is heat transfer coefficient within the residue (W m^{-1} C^{-1}); h_r is relative humidity within the residue elements; ρ_{vs}' is the saturated vapor density (kg m^{-3}) of the residue elements, given in Eqn. [93]; ρ_v is vapor density (kg m^{-3}) of the air within the residue layer; r_h is a boundary layer resistance (s m^{-1}) between residue elements and the air space within the residue layer; and R_n is the net downward radiation flux within the residue. This equation includes the assumption that residue elements and surrounding air voids within a layer are in thermal equilibrium.

Heat capacity

The volumetric heat capacity of residue is computed from the specific heat of residue and water, weighted according to their volumetric fractions and assuming the specific heat of air is negligible. It is calculated as

$$C_r = \rho_r (c_r + w_r c_l) \tag{56}$$

where ρ_r, c_r, and w_r are density, specific heat capacity (taken as 1900 J kg^{-1} C^{-1}), and gravimetric water content (kg kg^{-1}) of the residue, and c_l is the specific heat capacity of water (J kg^{-1} C^{-1}).

Thermal convection/conduction

Heat is transferred through the residue by conduction through residue elements and convection through air voids. The relative magnitude of these two processes depends on wind speed within the residue, and density and moisture content of the residue. Based on results from Kimball and Lemon (1971), Bristow et al. (1986) assumed that thermal convection through crop residue increases linearly with wind speed, but neglected the effect of residue density. The following equation was taken from Bristow et al. (1986) and modified for density of the residue:

$$k_v = k_a(1 + 0.007T)(1 + k_{rb}u_r)(1 - \rho_r / \rho_{rs})$$ [57]

where u_r is wind speed within the residue, ρ_{rs} is specific density of the residue, k_a is the thermal conductivity of still air, and k_{rb} is a parameter for the influence of windspeed at surface of residue layer on the transfer of heat and vapor through the residue layer with values ranging from 4.0 for wheat residue to 8.5 for larger residue elements such as corn stalks lying horizontal (Flerchinger et al, 2003). Wind speed at the surface of the residue is calculated assuming a logarithmic wind profile to the height of the residue or an exponentially decreasing profile within the plant canopy; wind speed within the residue is assumed to decrease linearly with depth to a value of zero at the soil surface.

Thermal conduction within the residue is dependent largely on moisture content and is calculated as a weighted average of the conductivities of residue and water:

$$k_t = k_{rs}(\rho_r / \rho_{rs}) + k_l w_r(\rho_r / \rho_l)$$ [58]

where k_{rs} is thermal conductivity of the residue material, k_l is thermal conductivity of water, and w_r is gravimetric water content of the residue. The total heat transfer coefficient of the residue, k_r, is the sum of the convection and conduction coefficients.

Latent heat of evaporation

Latent heat is required to evaporate liquid water from the residue elements to vapor within the air voids of the residue layer. The rate of evaporation depends on the vapor density within the void spaces and the water content of the residue. Details for evaporation from the residue is given subsequently in the section describing water flux within the residue.

Heat Transport Processes in the Soil

The state equation for temperature distribution in the soil matrix, considering convective heat transfer by liquid and latent heat transfer by vapor for a layer of freezing soil is given by:

$$C_s \frac{\partial T}{\partial t} - \rho_i L_f \frac{\partial \theta_i}{\partial t} = \frac{\partial}{\partial z}\left[k_s \frac{\partial T}{\partial z}\right] - \rho_l c_l \frac{\partial q_l T}{\partial z} - L_v\left(\frac{\partial q_v}{\partial z} + \frac{\partial \rho_v}{\partial t}\right)$$ [59]

where the terms (W m^{-3}) represent, respectively: specific heat term for change in energy stored due to a temperature increase; latent heat required to freeze water; net thermal conduction into a layer; net thermal advection into layer due to water flux; net latent heat evaporation within the soil layer. In the above equation, C_s and T are volumetric heat capacity (J kg^{-1}C^{-1}) and temperature (C) of the soil, ρ_i is density of ice (kg m^{-3}), θ_i is volumetric ice content (m^3 m^{-3}), k_s is soil thermal conductivity (W m^{-1} C^{-1}), ρ_l is density of water, c_l is specific heat capacity of water (J kg^{-1} C^{-1}), q_l is liquid water

flux (m s^{-1}), q_v is water vapor flux (kg m^{-2} s^{-1}), and ρ_v is vapor density (kg m^{-3}) within the soil.

Specific Heat

Volumetric heat capacity of soil, C_s, is the sum of the volumetric heat capacities of the soil constituents:

$$C_s = \sum \rho_j c_j \theta_j \qquad [60]$$

where ρ_j, c_j, and θ_j are the density, specific heat capacity and volumetric fraction of the jth soil constituent.

Latent Heat of Fusion

Due to matric and osmotic potentials, soil water exists in equilibrium with ice at temperatures below the normal freezing point of bulk water, and over the entire range of soil freezing temperatures normally encountered. A relation between ice content and temperature must therefore be defined before latent heat of fusion can be determined. The total potential of the soil water with ice present is controlled by the vapor pressure over ice, and is given by the freezing point depression equation (Fuchs et al., 1978):

$$\phi = \pi + \psi = \frac{L_f}{g}\left(\frac{T}{T_K}\right) \qquad [61]$$

where π is soil water osmotic potential (m), and ψ is soil matric potential. Osmotic potential in the soil is computed from

$$\pi = -cRT_K/g \qquad [62]$$

where c is solute concentration (eq kg^{-1}) in the soil solution. Given the osmotic potential, soil temperature defines the matric potential and, therefore, liquid water content. If the total water content is known, ice content and the latent heat term can be determined.

Thermal conduction

Thermal conductivity of the soil is calculated using the theory presented by De Vries (1963). A fairly moist soil is conceptualized as a continuous medium of liquid water with granules of soil, crystals of ice, and pockets of air dispersed throughout. The thermal conductivity of such an idealized model is expressed as

$$k_s = \frac{\sum m_j k_j \theta_j}{\sum m_j \theta_j} \qquad [63]$$

where m_j, k_j, and θ_j, are the weighting factor, thermal conductivity, and volumetric fraction of the jth soil constituent, i.e. sand, silt, clay, organic matter, water, ice and air. The method used for determining values for the weighting factor, m_j, is discussed by De Vries (1963).

Latent heat of vaporization

Net latent heat of vaporization occurring in a soil layer is computed from the rate of increase in vapor density minus the net vapor transfer into the layer. Vapor density in the soil is calculated assuming equilibrium with total water potential by:

$$\rho_v = h_r \rho_v' = \rho_v' \exp\left(\frac{M_w g}{RT_K}\phi\right) \qquad [64]$$

where ρ_v is vapor density (kg m^{-3}), ρ_v' is saturated vapor density, h_r is relative humidity, M_w is molecular weight of water (0.018 kg mole^{-1}), g is acceleration of gravity (9.81 m s^{-2}), R is universal gas constant (8.3143 J mole^{-1} K^{-1}), and φ is total water potential (m).

Water Fluxes Within the System

Water Flux Through the Canopy

Vapor flux through the canopy is written similarly to the canopy heat flux equation:

$$\frac{\partial \rho_v}{\partial t} = \frac{\partial}{\partial z}\left(k_e \frac{\partial \rho_v}{\partial z}\right) + E_l \qquad [65]$$

where the terms (kg s^{-1} m^{-3}) represent: net change in vapor contained within a layer; net vapor flux into a canopy layer; and a source term for transpiration/evaporation from the canopy elements leaves within the canopy layer. Here, E_l is transpiration or evaporation from the leaves within the canopy and other terms are defined previously.

Vapor transfer within the canopy

The transfer coefficient for vapor flux within the canopy, k_e, is assumed equal to that for heat transfer within the canopy and is described previously.

Vapor transfer from canopy elements

Vapor transfer for a given plant species within a canopy layer, $E_{l,i,j}$, is computed from

$$E_{l,i,j} = L_{AI,i,j} \frac{\rho_{vs,i,j} - \rho_{v,i}}{r_{s,i,j} + r_{v,i,j}} \qquad [66]$$

where $L_{AI,i,j}$ is the leaf area index, $\rho_{vs,i,j}$ and $\rho_{v,i}$ are vapor density (kg m^{-3}) of plant canopy elements (i.e. leaves) and of air within the canopy, $r_{s,i,j}$ is stomatal resistance per unit of leaf area index (s m^{-1}), $r_{v,i,j}$ is the resistance to water vapor (s/m) from the canopy leaves, and the subscripts refer to plant species j within canopy layer i. Resistance to water vapor transfer from the leaves is computed from (Campbell and Norman, 1998)

$$r_{v,i,j} = \frac{6.8P}{R(T_{c,i}+273.16)}\sqrt{\frac{d_{l,j}}{u_{c,i}}} \ . \qquad [67]$$

Evaporation from canopy elements

Evaporation within the canopy is computed for non-transpiring standing dead plant material and transpiring leaves with free water on the leaves (from dew formation or intercepted rainfall). In either case, evaporation is computed from Eqn. [66] with the stomatal resistance taken as zero. In the case of free water on the leaves, vapor density at the surface of the leaves is taken as the saturated vapor density for the computed leaf temperature. Vapor density of the standing dead plant material is computed from:

$$\rho_{vs} = h_r \rho_v' = \rho_v' \exp\left(\frac{M_w g}{RT_K}\psi\right) = \rho_v' \exp\left(\frac{M_w g}{RT_K} a_c w_c^{b_c}\right) \qquad [68]$$

16

where w_c is the water content (kg kg^{-1}) of the dead plant material, and a_c and b_c are coefficients with suggested values of -53.72 m and 1.32. Although the model accounts for interception and evaporation of precipitation within the canopy, it does not have provisions for melting intercepted snow and treats all intercepted precipitation as liquid.

Transpiration from canopy leaves

Plant stomates are assumed to close if light or temperature conditions are not adequate for transpiration. If incoming solar radiation, S_t, is less than 10 W m^{-2}, or if the air temperature T_a, is colder than a specified minimum air temperature, transpiration is set to zero and there is no vapor transfer through the stomates for the given plant species. However, evaporation of free water from the plant leaves may be considered as described in the previous section.

Transpiration within a canopy layer, $E_{l,i,j}$ (W m^{-2}), is determined assuming a soil-plant-atmosphere continuum. Water flow is calculated assuming continuity in water potential throughout the plants as illustrated in Figure 2 and may be calculated at any point in the plant from

$$T_j = \sum_{k=1}^{NS} \frac{\psi_k - \psi_{x,j}}{r_{r,j,k}} = \sum_{i=1}^{NC} \frac{\psi_{x,j} - \psi_{l,i,j}}{r_{l,i,j}} = \sum_{i=1}^{NC} \frac{\rho_{vs,i,j} - \rho_{v,i}}{r_{s,i,j} + r_{v,i,j}} L_{AI,i,j}$$ [69]

Here, T_j is total transpiration rate (kg m^{-2} s^{-1}) for plant species j; ψ_k, $\psi_{x,j}$ and $\psi_{l,i,j}$ are water potential (m) in layer k of the soil, in the plant xylem of plant species j, and in the leaves of canopy layer i; $r_{r,j,k}$ and $r_{l,i,j}$ are the resistance to water flow (m^3 s kg^{-1}) through the roots of soil layer k and the leaves of canopy layer i for plant species j; $\rho_{vs,i,j}$ and $\rho_{v,i}$ are the vapor density (kg m^{-3}) within the stomatal cavities (assumed to be saturated vapor density) of plant species j and of the air within canopy layer i; NS and NC are the number of soil and canopy nodes; and other terms are as described previously. Root resistance for each plant species within each soil layer is calculated by dividing total root resistance for the plant by its fraction of roots within the soil layer. Leaf resistance for each plant species within each canopy layer is computed from total leaf resistance for the plant based on its leaf area index within each canopy layer. Transpiration from the leaves of each plant species within each canopy layer, $E_{l,i,j}$, is computed from the last term in the above equation.
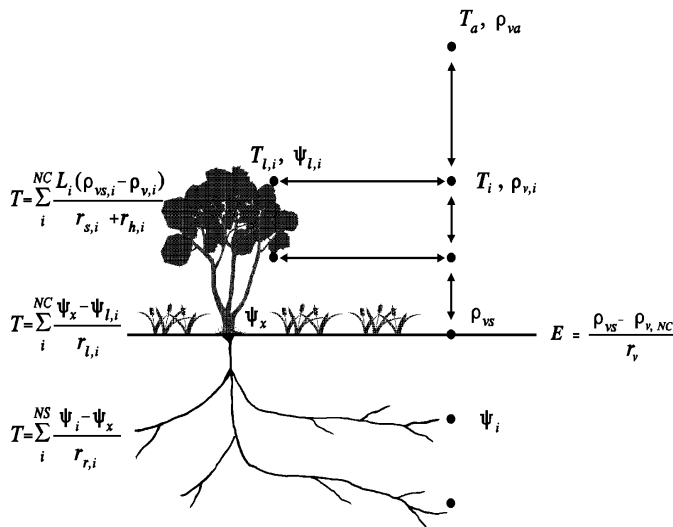

Figure 2: Physical representation of water flow through a plant in response to transpiration demands. (ρ_g is vapor density at the ground surface and r_v is resistance to vapor transfer within the canopy and equal to $\Delta z/k_e$; all other symbols are defined in the text.

Stomatal resistance, computed only as a function of leaf water potential in previous

17

versions of the model, was expanded in version 3.0 to generically include meteorological influences in a Stewart-Jarvis approach similar to that incorporated into the model by Link et al. (2004):

$$r_s = \left. r_{so}\left[1 + \left(\frac{\psi_l}{\psi_c}\right)^{n_s}\right] \middle/ f_{St}f_Tf_{VPD} \right. \qquad [70]$$

Here r_s is computed stomatal resistance, r_{so} is stomatal resistance with no stress, ψ_l is leaf water potential computed based on water flow along a water potential gradient through the soil-plant atmosphere continuum (Flerchinger et al. 1998), ψ_c is a critical water potential at which stomatal resistance is twice its minimum value, n_s is an empirical exponent, and f_{St}, f_T, and f_{VDP} are stomatal restriction factors for ambient solar radiation, temperature and vapor pressure deficit. Functions for f_{St} and f_T follow a Jarvis-Stewart approach (Jarvis, 1976; Stewart, 1988):

$$f_{St} = S_{t,i}\frac{(1000 + K_{St})}{1000(S_{t,i} + K_{St})} \qquad [71]$$

$$f_T = \frac{(T_i - T_L)(T_H - T_i)^{n_T}}{(T_{opt} - T_L)(T_H - T_{pot})^{n_T}} \qquad [72]$$

where $S_{t,i}$ is the total solar radiation incident on canopy layer i, T_L is leaf temperature, T_i is temperature of layer i, K_{St} is a parameter to control the influence of solar radiation, T_L and T_H are the lower and upper temperature limit for transpiration, T_{Opt} optimum temperature for transpiration, and

$$n_T = \frac{(T_H - T_{opt})}{(T_{opt} - T_L)} \ . \qquad [73]$$

The form used for f_{VPD} follows that used by Link et al. (2004):

$$f_{VPD} = K_{VPD} + (1 - K_{VPD})r^{VPD} \qquad [74]$$

where K_{VPD} is the maximum reduction in stomatal conductance due to vapor pressure deficit, r is a coefficient for stomatal conductance due to vapor pressure deficit and VPD is the vapor pressure deficit (kPa) of the air within canopy.

Mass Balance of the Snowpack

Density and ice content of each snow layer are assumed constant during each time step while the change in liquid content is computed from the energy balance. At the end of the time step, the thickness and density of each layer are adjusted for vapor transfer and change in liquid content. Excess liquid water is routed through the snowpack using attenuation and lag coefficients to determine snowcover outflow, and density of the snow is adjusted for compaction and settling.

Snowcover outflow

The amount of liquid water that can be held in the snow due to capillary tension is computed from

$$w_{sp_{hold}} = w_{sp_{min}} + \left(w_{sp_{max}} - w_{sp_{min}}\right)\frac{\rho_e - \rho_{sp}}{\rho_e} \text{ for } \rho_{sp} < \rho_e \qquad [75]$$

where $w_{sp,min}$ is the minimum value water holding capacity (m^3 m^{-3}) and applies to dense, ripe

snowpacks, $w_{sp,max}$ is the maximum value of w_{sp}, and ρ_e is the snow density (kg m^{-3}) corresponding to $w_{sp,min}$. The permeability of snow is quite variable and not well defined. Therefore, after the water holding capacity of the snowpack is satisfied, excess liquid water is lagged and attenuated using empirical equations. The maximum lag in hours for snowcover of depth d_{sp} (m) is

$$L_{w\max} = C_{L1}\left[1 - \exp(-250 d_{sp}/\rho_{sp})\right] \qquad [76]$$

where C_{L1} is the maximum allowable lag (taken to be 10 hours; Anderson, 1976). The actual lag depends on the amount of excess liquid water and is determined by

$$L_w = \frac{L_{w\max}}{100 C_{L2} W_x + 1} \qquad [77]$$

where W_x is the depth of excess liquid water (m), and C_{L2} is an empirical coefficient (assigned to 1.0 cm^{-1}). After the excess liquid water is lagged, it is attenuated and snowcover outflow is calculated from

$$W_o = \frac{S_{sp} + W_L}{1 + C_{L3}\exp\left[C_{L4} W_L \rho_{sp}/(\rho_l d_{sp})\right]} \qquad [78]$$

where W_L is the depth of lagged excess water (m), S_{sp} is the excess water in storage (m), and C_{L3} (5.0 hr) and C_{L4} (450, dimensionless) are empirical coefficients.

Density change of snowcover

Snow density changes over time due to compaction, settling, and vapor transfer. Compaction and settling of the snow are discussed in the following sections, while vapor transfer was discussed previously.

Compaction of the snow

Snow deforms continuously and permanently when a sustained load is applied. A basic equation describing the rate at which snow will deform in response to a load may be written as (Anderson, 1976)

$$\frac{1}{\rho_{sp}}\frac{\partial \rho_{sp}}{\partial t} = C_1 W_{sp}\exp\left(0.08T - C_2 \rho_{sp}/\rho_l\right) \qquad [79]$$

where W_{sp} is the weight of snow (expressed in terms of centimeters of water equivalent) above the layer of snow, C_1 is the hourly fractional increase in density per load of water-equivalent (taken as 0.01 cm^{-1}hr^{-1}), C_2 is an empirical coefficient (approximately 21.0), and T is snow temperature (C).

Settling of the snow

After snow falls, metamorphosis of the ice crystals in the snowpack as they change shape causes the pack to settle. This process is relatively independent of snow density up to a value, ρ_d, of about 150 kg m^{-3}. Anderson (1976) suggested the following relation for fractional increase in density due to settling:

$$\frac{1}{\rho_{sp}}\frac{\partial \rho_{sp}}{\partial t} = \begin{array}{ll} C_3\exp(C_4 T) & \text{for } \rho_{sp} < \rho_d \\ C_3\exp(C_4 T)\exp\left[-46(\rho_{sp} - \rho_d)\right] & \text{for } \rho_{sp} > \rho_d \end{array} \qquad [80]$$

where C_3 is the fraction rate of settling at 0°C for densities less than ρ_d, and C_4 is an empirical coefficient (taken as 0.04 °C). The presence of liquid water will increase the rate of settling.

When liquid water is present in the snow, the fractional rate of settling computed from this equation is multiplied by a factor, C_5 (assumed equal to 2.0; Anderson, 1976).

Water Flux Through the Residue

Vapor flux through the residue is described by

$$\frac{\partial \rho_v}{\partial t} = \frac{\partial}{\partial z}\left(K_v \frac{\partial \rho_v}{\partial z}\right) + \frac{\partial}{\partial z}\left(\frac{(h_r \rho'_{vs} - \rho_v)}{r_h}\right) \qquad [81]$$

where the terms represent, respectively: change in vapor density within the residue layer, net vapor flux into a residue layer, and evaporation rate from the residue elements. Here, ρ_v is vapor density (kg m^{-3}) of the air space within the residue; K_v is the convective vapor transfer coefficient within the residue (m s^{-2}), taken as $k_v/\rho_a c_a$ where ρ_a and c_a the density and specific heat capacity of air; h_r is the relative humidity within the residue elements; ρ_{vs}' is saturated vapor density at the temperature of the residue elements; and r_h is the resistance (s m^{-1}) to vapor transfer between the residue elements and the air voids within the residue layer.

Evaporation within the residue

Evaporation from the residue elements depends on humidity or water potential of the water held by the residue elements. Relative humidity of the residue elements is determined from water potential of the residue by

$$h_r = \exp\left(\frac{M_w g}{RT_K}\psi\right) = \exp\left(\frac{M_w g}{RT_K}a_r w_r^{b_r}\right) \qquad [82]$$

where w_r is water content of the residue. Typical values for the empirical coefficient a_r and b_r for wheat straw are -53.72 m and 1.32, respectively (Myrold et. al., 1981).

Suggested values for resistance to vapor transfer between residue elements and air voids, r_{vr}, is 1000-50,000 s m^{-1}. (Potential modification to the model may include calculation of r_{vr} from windspeed within the residue.)

Water Flux Through the Soil

The soil water flux equation for with provisions for freezing and thawing soil is written as:

$$\frac{\partial \theta_l}{\partial t} + \frac{\rho_i}{\rho_l}\frac{\partial \theta_i}{\partial t} = \frac{\partial}{\partial z}\left[K\left(\frac{\partial \psi}{\partial z}+1\right)\right] + \frac{1}{\rho_l}\frac{\partial q_v}{\partial z} + U \qquad [83]$$

where the terms (m^3 m^{-3} s^{-1}) represent, respectively: change in volumetric liquid content; change in volumetric ice content; net liquid flux into a layer; net vapor flux into a layer; and a source/sink term for water extracted by roots;. In this equation, K is unsaturated hydraulic conductivity (m s^{-1}), ψ
is soil matric potential (m), and U is a source/sink term for water flux (m^3 m^{-3} s^{-1}).

Liquid flux

Liquid water flow is computed from the hydraulic conductivity, and matric and

20

gravitational potential gradient in the soil, as shown in Eqn. [83]. Water flow in frozen soil is assumed analogous to that in unsaturated soil (Cary and Mayland, 1972; and Miller, 1963). Therefore, the relationships for matric potential and hydraulic conductivity of unsaturated soils are assumed valid for frozen soils. However, hydraulic conductivity computed from the particular form of the soil moisture release curve below is reduced linearly with ice content assuming zero conductivity at an available porosity of 0.13 (Bloomsburg and Wang, 1969). To avoid numerical problems upon thawing, the model limits water flux into any layer so as not to exceed θ_s, however water content can exceed θ_s as water present within a soil layer freezes and expands.

Matric potential for unsaturated conditions is computed from soil water content through the soil moisture release curve. Several options are available in the model for estimating the soil moisture release curve, including the Campbell equation (Campbell, 1974), the Brooks-Corey relation (Brooks and Corey, 1966), and the van Genuchten equation. These equations are given below. Once water content reaches saturation (θ_s), matric potential may exceed the air entry potential and is independent of water content.

Campbell Equation:
    The Campbell equation takes the form

$$\psi = \psi_e \left(\frac{\theta_l}{\theta_s} \right)^{-b} \qquad [84]$$

where ψ_e is air entry potential (m), b is a pore size distribution parameter, and θ_s is saturated water content ($m^3 m^{-3}$). Unsaturated hydraulic conductivity is computed from

$$K = K_s \left(\frac{\psi_e}{\psi} \right)^{(2+3/b)} \qquad [85]$$

for $\psi < \psi_e$, where K_s is saturated hydraulic conductivity ($m\ s^{-1}$) .

Brooks-Corey Equation:
    The Brooks-Corey relation for the soil moisture release curve is written as

$$\psi = \psi_e \left(\frac{\theta - \theta_r}{\theta_s - \theta_r} \right)^{-1/\lambda} \qquad [86]$$

where θ_r is the residual water content and λ is the Brooks-Corey pore size distribution parameter (not to be confused with that in the Campbell equation). Unsaturated conductivity for the Brooks-Corey equation is computed from

$$K = K_s \left(\frac{\psi}{\psi_e} \right)^{-\lambda(l+2)+2} . \qquad [87]$$

Here, l is a pore-connectivity parameter, assumed to be 2.0 in the original study of Brooks and Corey (1964).

Van Genuchten Equation:
    The Brooks-Corey relation for the soil moisture release curve is written as

21

$$\psi = -\frac{1}{\alpha}\left[\left(\frac{\theta-\theta_r}{\theta_s-\theta_r}\right)^{-1/m}-1\right]^{\frac{1}{n}} \qquad [88]$$

where α, m, and n are all empirical coefficients affecting the shape of the soil moisture release curve. The value of m is restricted to $m=1-1/n$ as the Mualem model is assumed for liquid water flow in the SHAW model when using the van Genuchten equation. Hydraulic conductivity is computed from

$$K = \frac{K_s\left\{1-|\alpha\psi|^{mn}\left[1+|\alpha\psi|^n\right]^{-m}\right\}^2}{[1+|\alpha\psi|^{n^n}]^{ml}} \qquad [89]$$

for $\psi < 0$. Air entry potential ψ_e is taken as zero in the van Genuchten equation.

Vapor flux

      Vapor transfer in the soil is calculated as the sum of the gradient in vapor density due to a water potential gradient, q_{vp}, and that due to a temperature gradient, q_{vT} (Campbell, 1985), where

$$q_v = q_{vp} + q_{vT} = -D_v\rho'_v\frac{dh_r}{dz} - \zeta\, D_v h_r s_v\frac{dT}{dz}. \qquad [90]$$

Here D_v is vapor diffusivity (m^2 s^{-1}) in the soil, h_r is relative humidity within the soil, s_v is the slope of the saturated vapor pressure curve ($d\rho_v'/dT$ in kg m^{-3}C^{-1}), and ζ is an enhancement factor. Vapor density in the soil is related to vapor diffusivity in air by

$$D_v = D'_v\, b_v\, \theta_a^{c_v} . \qquad [91]$$

Here, D_v' is diffusivity of water vapor in air, θ_a is air porosity, and b_v and c_v coefficients accounting for the tortuosity of the air voids with values of 0.66 and 1.0, respectively (Campbell, 1985). Observed vapor transfer in response to a temperature gradient exceeds that predicted by Eqn. [90], therefore an enhancement factor is included, which is calculated from (Cass et al., 1984)

$$\zeta = E_1 + E_2(\theta_l/\theta_s) - (E_1 - E_4)\exp\left(-(E_3\theta_l/\theta_s)^{E_5}\right) \qquad [92]$$

where E_1, E_2, E_4 and E_5 have assigned values of 9.5, 3.0, 1.0, and 4.0, respectively. E_3 is calculated from clay content by $\theta_s(1 + 26(\%\text{clay})^{-1/2})$.

      A seventh-order polynomial is used approximate the saturated vapor density from temperature, given by

$$\rho'_v = \frac{100}{RT_K}\left(\begin{array}{l}6.1104546 + 0.4442351\,T + 0.014302099\,T^2 + 2.6454708\times10^{-4}T^3 \\ +3.0357098\times10^{-6}\,T^4 + 2.0972268\times10^{-8}\,T^5 + 6.0487594\times10^{-11}\,T^6 - 1.469687\times10^{-13}\,T^7\end{array}\right) \qquad [93]$$

The slope of the saturated vapor density curve is expressed very accurately for typical temperature ranges using the empirical equation given by

$$s_v = 0.0000165 + 4944.43\rho'_v/T_K^2. \qquad [94]$$

Above 45°C, however, this function diverges somewhat from the derivative of Eqn. [93], in which case the derivative of Eqn. [93] is used for the slope of the saturated vapor density curve.

Ice content

Unknowns in Eqns. [59], [83], and [84] are temperature, water content, ice content, and matric potential so an additional equation is needed for a solution. This is provided by the Clausius-Clapeyron equation. When ice is present, total water potential is equal to the matric potential and is related to temperature by (Fuchs et al. 1978):

$$\phi = \pi + \psi = \frac{L_f}{g}\left(\frac{T}{T_K}\right)$$ [95]

where g is the acceleration of gravity (m s^{-2}) and π is osmotic potential (m). Thus, as temperature drops, water potential becomes more negative, creating a gradient in water potential and causing moisture movement toward the freezing front. Based on Eqn. [95], positive matric potentials cannot exist when ice is present in a soil layer. Osmotic potential within the soil is computed from

$$\pi = -cRT_K/g$$ [96]

where c is solute concentration (eq kg^{-1}) in the soil solution. From Eqns. [84], [95], and [96], liquid water content is defined by temperature during freezing conditions; soil water content greater than that computed from these relations is assumed to be ice.

Solute Fluxes

The SHAW model accounts for solute absorption by the soil matrix, and considers three processes of solute transfer: molecular diffusion, convection, and hydrodynamic dispersion. The transient, solute flux equation may be written as:

$$\rho_b\frac{\partial S}{\partial t} = \rho_l\frac{\partial}{\partial z}\left((D_H + D_m)\frac{\partial c}{\partial z}\right) - \rho_l\frac{\partial(q_l c)}{\partial z} - \rho_b V$$ [97]

where the terms (eq m^{-3}s^{-1}) represent: rate of change of total solute in a soil layer; net solute flux due to combined effects of diffusion and dispersion; net solute flux due to convection; and a sink term for loss of solutes by degradation and root extraction. Here, ρ_b is soil bulk density (kg m^{-3}), S is total solutes present per mass of soil (eq kg^{-1}); D_H is the hydrodynamic dispersion coefficient (m^2 s^{-1}), D_m is the molecular diffusion coefficient (m^2 s^{-1}); q_l is liquid water flux (m s^{-1}); c is solute concentration in soil solution (eq kg^{-1}); and V is a sink term for solute degradation and extraction by roots (eq kg^{-1}s^{-1}). Several types of solutes may be modeled simultaneously with the SHAW model, however solutes are assumed to be non-interacting with other solutes.

Molecular diffusion

Diffusion of solutes through soil is affected by moisture content and tortuosity, and is related to that in free water by (Campbell, 1985; and Bolz and Tuve, 1976)

$$D_m = D_o \tau \theta_l^3 (T_K/273.16)$$ [98]

where D$_o$ is the diffusion coefficient of a given solute in water at 0°C (m^2 s^{-1}) and τ is a

soil-dependent constant for tortuosity.

Solute convection

Solute convection by moisture movement can occur only in the direction of moisture flow and is proportional to moisture flux and solute concentration. Calculation of solute transport by convection alone assumes uniform velocity in all pores and therefore does not account for dispersion of salts. Dispersion of solutes due to nonuniform velocity is accounted for in the hydrodynamic dispersion coefficient.

Solute dispersion

Solutes are transported by convection at the mean velocity of moisture flow, but are dispersed about the mean velocity due to differences in velocity between and within soil pores. The hydrodynamic dispersion coefficient depends on the average flow velocity and is calculated from (Bresler, 1973)

$$D_H = \kappa \, q_l / \theta_l \qquad\qquad [99]$$

where κ is a soil-dependent constant (m).

Solute sink terms

Solute of a given type can be lost from the soil by degradation or extraction by roots. Solute degradation, if specified by the user, is assumed to follow an exponential decay. Solute degradation for a time step Δt (s) is computed from:

$$V = S\left[1 - \exp\left(\frac{\Delta t \ln(0.5)}{86{,}400 \, t_{1/2}}\right)\right] \qquad\qquad [100]$$

where $t_{1/2}$ is the half-life (d) of the solute. Solute extraction from the soil by roots is assumed non-selective and equal to the concentration of solutes within the soil solution extracted by the roots.

Solute absorption

A linear absorption equation is assumed for the equilibrium balance between solute concentration in the soil solution and that absorbed onto the soil matrix. The relation is expressed as

$$S = \left(K_d + \frac{\rho_l \theta_l}{\rho_b}\right) c \qquad\qquad [101]$$

where K_d is partitioning coefficient between the soil matrix and the soil solution (kg kg^{-1}). For a completely mobile solute (not absorbed by the soil), $K_d = 0$. A typical value of K_d for phosphorus, an ion strongly absorbed to the soil, is approximately 60 kg kg^{-1} (Campbell, 1985).

Lower Boundary Conditions

Several options are available for specifying the conditions for heat and water flux at the lower boundary. Soil temperature and water content at the lower boundary may be either

specified by the user or model-estimated. User-specified temperature and water content at the lower boundary are input through the temperature and water input files. The model linearly interpolates between input values on different dates to obtain the temperature or water content at the lower boundary for each time step. Thus, at least two input profiles (the initial profile and another on or beyond the last day of simulation) are required for user-specified temperature or water content.

If model-estimated soil water content at the lower boundary is specified, the gradient for water flux at the lower boundary is assumed to be due to gravity alone. Under this assumption, the matric potential gradient term in Eqn. [83] becomes zero, leaving the gravity term, which is unity. Thus, this lower boundary condition is sometimes referred to as a unit gradient. Water flux is equal to the unsaturated hydraulic conductivity for the existing water content at the lower boundary.

The model will optionally estimate soil temperature at the lower boundary for each time step based on either: no conductive heat flux at the lower boundary, or the soil temperature response above the lower boundary and an assumed constant temperature deep within the soil profile. For the no-heat-flux lower boundary, the model simply sets the lower boundary temperature equal to the temperature of the node above it. Alternatively, the model will estimate end-of-time-step lower boundary temperature based on the force-restore approach described by Hirota et al. (2002). They present the following expression for the ground surface:

$$\left(1+\frac{2z}{d_d}\right)\frac{\partial T}{\partial t}=\frac{2}{C_s d_d}G-\omega(T-T_{AVG})$$ [102]

where z is the depth (m) below the surface, ω is the frequency (s^{-1}) of fluctuation period (diurnal or annual), d_d is damping depth (m) corresponding to ω, and T_{AVG} is the average soil surface temperature for the oscillation. Applying this equation to a finite depth above the lower boundary, expressing it in finite difference terms, and solving it for end-of-time-step temperature yields:

$$T_{NS}^{j+1}=T_{NS}^{j}-\frac{\Delta t}{\left(1+\frac{2(z_{NS}-z_{NS-1})}{d_d}\right)}\left[\frac{2k_s}{C_s d_d(z_{NS}-z_{NS-1})}\left(T_{NS}^{j}-T_{NS-1}^{j}\right)+\omega\left(T_{NS}^{j}-T_{AVG}\right)\right]$$ [103]

Here, subscripts *NS* and *NS-1* denote the bottom soil layer and the layer above it, and superscripts denote beginning (j) and end ($j+1$) of time step values, Δt is the time step (s), and z_{NS} is depth of the bottom soil node, *NS*. Due to its assumptions, Equation [102] is not appropriate for large temperature gradients (Hirota et al. 2002). For model application therefore, it is best if the lower boundary is below the diurnal damping depth (approximately 50 cm for most soils). The annual damping depth is therefore used in Eqn. [103], which is expressed as

$$d_d=\left(\frac{2k_s}{C_s\omega}\right)^{1/2}$$ [104]

Here, ω is the radial frequency (1.99238×10^{-7} s^{-1}) of the annual temperature oscillation, equal to $2\pi/\Delta t$. T_{AVG} is the average annual soil temperature, taken to be a constant soil temperature deep within the soil profile. It may be closely approximated by the annual average air temperature.

Precipitation and Infiltration

Precipitation and snowmelt are computed at the end of each time step after the heat, water and solute fluxes are computed for the time step. Moisture and temperature conditions of the plant canopy, snow, residue and soil are adjusted for absorption, interception and infiltration of rainfall or snowmelt.

Snow Accumulation

Precipitation is assumed to be snow if one of two conditions exist: 1) the air temperature or optionally the wet-bulb air temperature is below a specified temperature; or 2) a non-zero value for snow density is input for the time step in the weather input file. If temperature indicates snow but density is unknown, newly fallen snow density (kg m^{-3}) is estimated by (Anderson, 1976)

$$\rho_{sp} = 50 + 1.7(T_{wb} + 15)^{1.5}$$ [105]

where T_{wb} is wet-bulb temperature (C).

When snow falls on bare soil or residue, sufficient snow is melted to reduce the surface residue or soil node to 0°C. Additional snow is divided into layers of a defined thickness (approximately 2.5 cm for surface layers). New snow falling on existing snow is allowed to fill the surface snow layer to the defined thickness. Properties of the resulting layer are the weighted average of new and existing snow. Moisture and energy from rain falling on snow are included in the mass balance calculation of the surface layer.

Interception by Canopy and Residue

The maximum fraction of precipitation (or snowmelt in the case of the residue layer) intercepted by the canopy or residue is equal to the fraction of surface covered by plants or residue when viewed vertically downward. This is defined by computing τ_b (Eqns. [9] and [18]) with an incident angle (β) of 90°. However, interception is limited to a maximum depth of water on the leaves of the plant canopy and the maximum water content of the residue. Interception depth per unit of leaf area for transpiring plants is input by the user; intercepted water is ultimately lost to evaporation. Standing or flat plant residue can intercept water up to a maximum water content (assumed equal to the water content defined by 99.9% relative humidity in the residue).

Infiltration into Soil

Rainfall, snowmelt and ponded water are infiltrated into the soil at the end of each time step. Infiltration is calculated using a Green-Ampt approach for a multi-layered soil. The infiltration rate as a wetting front passes through layer m of a multi-layered may be written as

$$f = \frac{dF'_m}{dt'} = \frac{F'_m/\Delta\theta_l + \psi_f + \sum\Delta z_k}{\dfrac{F'_m}{\Delta\theta_l K_{e,m}} + \sum\dfrac{\Delta z_k}{K_{e,k}}}$$ [106]

where f is infiltration rate (m s^{-1}), $K_{e,k}$ is the effective hydraulic conductivity of layer k (m s^{-1}), ψ_f

is the suction head (m) at the wetting front and is assumed numerically equal to the matric potential of the layer, $\Delta\theta_l$ is the change in water content as the wetting front passes, F'_m is the accumulated infiltration (m) into layer m, t' is the time (s) since the wetting front entered layer m, and $\Sigma\Delta z_k$ is the depth (m) to the top of layer m. Effective hydraulic conductivity for infiltration is determined by substituting the effective porosity, computed from ($\theta_s - \theta_i$), for θ_l in Eqn. [85]. Conductivity is then reduced linearly depending on ice content and assuming zero conductivity at an available porosity of 0.13 (Bloomsburg and Wang 1969). The above equation may be integrated and written in dimensionless form as

$$t_* = (z_* - 1)\ln(1 + F_*) + F_*$$ [107]

where

$$f_* = \frac{f}{K_{e,m}}$$ [108]

$$F_* = \frac{F_{m'}}{\Delta\theta_l(\psi_f + \Sigma\Delta z_k)}$$ [109]

$$t_* = \frac{K_{e,m}t'}{\Delta\theta_l(\psi_f + \Sigma\Delta z_k)}$$ [110]

$$z_* = \frac{K_{e,m}}{\psi_f + \Sigma\Delta z_k}\sum_{k=1}^{m-1}\frac{\Delta z_k}{K_{e,k}}$$ [111]

Eqn. [107] is implicit with respect to F_*. By expanding the logarithmic term in to a power series, Flerchinger and Watts (1987) developed the following explicit expression for F_*:

$$F_* = \frac{1}{2}\left(t_* - 2z_* + \sqrt{(t_* - 2z_*)^2 + 8t_*}\right)$$ [112]

This expression is valid only if nearly-saturated flow exists behind the wetting front, which was shown to occur only if $z_* \leq 1$. When this criteria is not met, infiltration is calculated using Darcy's equation and assuming zero matric potential at the wetting front.

Rainfall or snowmelt in excess of the calculated interception and infiltration is ponded at the surface until a specified maximum depth of ponding is satisfied, after which runoff occurs. Adjustments for leaching of solutes, melting of ice and freezing any infiltrated water is addressed in the following subsections.

Solute Leaching

Molecular diffusion and hydrodynamic dispersion are neglected for solute transport and leaching upon infiltration. With these simplifications, the solute balance equation during infiltration becomes

$$\rho_b \frac{\partial S}{\partial t} = -\rho_l \frac{\partial (q_l c)}{\partial z}$$

$$\rho_b (S' - S) = \frac{\rho_l F'_{k+1}}{\Delta z_k}\left[c_{avg} - \eta c' - (1-\eta)c\right] \qquad [113]$$

$$= \frac{\rho_l F'_{k+1}}{\Delta z_k}\left[c_{avg} - \frac{\eta S' + (1-\eta)S}{K_d + \theta_l \rho_l / \rho_b}\right]$$

where F'_{k+1} is the total water passing through layer k, c_{avg} is the average concentration of water entering the layer, S' and c' are total salts and solute concentration present in the layer after leaching, and η is a weighting factor for end-of-time-step values. Total salts in the layer after leaching can be solved directly by

$$S' = \frac{\rho_l F'_{k+1} c_{avg} / \Delta z_k + S\left(\rho_b - \dfrac{\rho_l(1-\eta)F'_k}{(K_d + \theta_l \rho_l / \rho_b)\Delta z_k}\right)}{\rho_b + \dfrac{\rho_l \eta F'_k}{(K_d + \theta_l \rho_l / \rho_b)\Delta z_k}} \qquad [114]$$

This equation assumes moisture movement is steady state and moisture content in the layer is not changing. Therefore, S must be adjusted for the solutes entering the layer as water fills the pores prior to applying this equation.

Energy calculations

Heat carried by the infiltrating water affects the temperature and ice content of the soil. If the soil is frozen, infiltrating water may cause some ice to melt, or the infiltrating water may freeze depending on the temperature of the water and soil. The final temperature and ice content of a soil layer is calculated using conservation of energy by

$$\rho_l c_l F'_k (T_{F_k} - T') = C_s (T' - T) - \rho_l L_f (\theta'_i - \theta_i) \qquad [115]$$

where $T_{F,k}$ is the temperature (C) of the water entering layer k; T' and θ_i' are the temperature (C) and ice content (m^3 m^{-3}) of the layer after infiltration; and all water draining out of layer k is at temperature T'. If θ_i' is known to be greater than or equation to zero, T' can be solved directly. Otherwise, ice content is a function of the total water content and final temperature. In this case, T' is initially assumed equal to the freezing point of water in the soil, which is calculated from

$$T_{frz} = 273.16\left(\frac{\phi}{(L_f / g) - \phi}\right) \qquad [116]$$

where φ is total water potential if all water is liquid. Ice content θ_i' is then estimated using Eqn. [115]. Liquid content θ_l, matric potential ψ, concentration of soil solution c, and total water potential φ are determined from the estimated ice content and total water content. With this information, the temperature T' and a second approximation of ice content is calculated. These updated values are sufficiently close to the true values required for energy balance because the specific heat term in Eqn. [116] is quite small compared to the latent heat term.

Numerical Implementation

The one-dimensional state equations presented describe energy, water and solute balance for infinitely small layers. The energy and water balance equations for layers within the plant canopy, snow residue and soil are written in implicit finite difference form and solved using an iterative Newton-Raphson technique. Finite difference approximation enables us to apply these equations to nodes representing layers of finite thickness. Flux between nodes is calculated assuming linear gradients. Energy storage for each node is based on layer thickness. A balance equation is written in terms of unknown end-of-time step values within the layer and its neighboring layers. Partial derivatives of the flux equations with respect to unknown end-of-time step values are computed, forming a tri-diagonal matrix from which the Newton-Raphson approximations for the unknown values are computed. Iterations are continued until successive approximations are within a prescribed tolerance defined by the user.

The solution for each time step involves alternating back and forth between a Newton-Raphson iteration for the heat flux equations and one for the water flux equations. An iteration is conducted for the heat flux equations and temperature estimates (water content in the case of melting snow) for the end of the time step are updated. This is followed by an iteration for the water flux equations, where updated vapor density within the canopy and residue, matric potential in unfrozen soil layers, and ice content in frozen soil layers are determined. Upon completion of the iteration for the water flux equations, the solution reverts back to an iteration for the heat flux equations with the updated values. Iterations continue until subsequent iterations of both heat and water flux equations for each layer are within a prescribed tolerance. Thus, the heat and water flux equations are solved simultaneously, maintaining a correct balance between the two coupled equations.

After iterations for the heat and water flux equations have reached convergence, solute transport is computed using liquid fluxes from the water balance calculations. If more than one iteration is required for energy and water balance convergence, it is likely that there was sufficient moisture movement to affect solute concentrations, and the newly-calculated solute concentrations will be significantly different from those used in the energy and water balance calculations. In this case, the program returns to the energy and water balance calculations with the new solute concentrations and iterates until convergence is met.

References

Anderson, E.A. 1976. A point energy and mass balance of a snow cover. *NOAA Tech. Rep. NWS 19*, U.S. Department of Commerce, National Oceanic and Atmosphere Administration, National Weather Service, Silver Spring, MD. 150 p.

Bloomsburg, G.L. and S.J. Wang. 1969. Effect of moisture content on permeability of frozen soils. Paper presented at 16th annual meeting of Pacific Northwest Region, American Geophysical Union. 11pp.

Bolz, R.E. and G.L. Tuve (eds.). 1976. *Handbook of Tables for Applied Engineering Science, Second Edition.* The Chemical Rubber Co., Cleveland Ohio. 1166 p.

Bresler, E. 1973. Simultaneous transport of solutes and water under transient unsaturated flow conditions. Water Resour. Res. 9(4):975-986.

Bristow, K.L., G.S. Campbell, R.I. Papendick and L.F. Elliott. 1986. Simulation of heat and moisture transfer through a surface residue-soil system, Agric. and Forest Met., 36:193-214.

Brooks, R.H. and A.T. Corey. 1966. Properties of porous media affecting fluid flow. J. Irrig. and Drain Div., ASCE. 92(IR2):61-88.

Campbell, G.S. 1977. An Introduction to Environmental Biophysics. Springer-Verlag, New York, New York, 159 pp.

Campbell, G.S. 1985. Soil Physics with BASIC: Transport models for soil-plant systems. Elsevier, Amsterdam, 150 pp.

Campbell, G.S. and J.M. Norman. 1998. An Introduction to Environmental Biophysics, Second Edition, Springer, New York, New York, 1998.

Cary, J.W. and H.F. Mayland. 1972. Salt and water movement in unsaturated frozen soil. Soil Sci. Soc. Amer. Proc. 36:549-555.

Cass, A., G.S. Campbell, and T.L. Jones. 1984. Enhancement of thermal water vapor diffusion in soil. Soil Sci. Soc. Amer. Jour. 48:25-32.

Denmead, O.T. and E.F. Bradley. 1985. Flux-gradient relationships in a forest canopy. pp. 412-442 In: B.A. Hutchison and B.B. Hicks, The Forest-Atmosphere Interaction. D. Reidel Publishing Co., Hingham, Massachusettes.

De Vries, D.A. 1963. Thermal properties of soil. Chapter 7 In: W.R. Van Wijk (ed.), *Physics of Plant Environment*. North-Holland Publising Co., Amsterdam.

Dolman, A.J. 1993. A multiple source land surface energy balance model for use in GCMs'. Agric. and Forest Meteor., 65:21-45.

Dolman, A.J. and J.S. Wallace. 1991. Langrangian and K-theory approaches in modelling evaporation and sparse canopies. Q.J.R. Meteorol. Soc. 117:1325-1340.

Flerchinger, G.N. and F.J. Watts. 1987. Predicting infiltration parameters for a road sediment model. Trans. of ASAE 30(6):1700-1705.

Flerchinger, G.N. and K.E. Saxton. 1989. Simultaneous heat and water model of a freezing snow-residue-soil system I. Theory and development. Trans. of ASAE 32(2):565-571.

Flerchinger, G.N. and F.B. Pierson. 1991. Modeling plant canopy effects on variability of soil temperature and water. Agric. and Forest Meteor. 56(1991):227-246.

Flerchinger, G.N., J.M. Baker, and E.J.A. Spaans. 1996a. A test of the radiative energy balance of the SHAW model for snowcover. Hydrol. Proc. 10:1359-1367.

Flerchinger, G.N., C.L. Hanson and J.R. Wight. 1996b. Modeling evapotranspiration and surface energy budgets across a watershed. Water Resour. Res. 32(8):2539-2548.

Flerchinger, G.N. and F.B. Pierson. 1997. Modeling plant canopy effects on variability of soil temperature and water: Model calibration and validation. J. Arid Environ. 35:641-653.

Flerchinger, G.N., W.P. Kustas and M.A. Weltz. 1998. Simulating Surface Energy Fluxes and Radiometric Surface Temperatures for Two Arid Vegetation Communities using the SHAW Model. J. Appl. Meteor. 37(5):449-460.

Flerchinger, G.N., T.J. Sauer, and R.A. Aiken. 2003. Effects of crop residue cover and architecture on heat and water transfer at the soil surface. Geoderma 116(1-2):217-233.

Flerchinger, G.N. and Q. Yu. 2007. Simplified expressions for radiation scattering in canopies with ellipsoidal leaf angle distributions. Agric & Forest Meteor. 144:230-235.

Flerchinger, G.N., W. Xaio, D. Marks, T.J. Sauer, and Q. Yu. 2009a. Comparison of algorithms for incoming atmospheric long-wave radiation, Water Resour. Res., 45, W03423, doi:10.1029/2008WR007394.

Flerchinger, G.N., W. Xaio, T.J. Sauer, and Q. Yu. 2009b. Simulation of within canopy radiation exchange. NJAS – Wageningen Journal of Life Sciences 57:5-15.

Flerchinger, G.N., M.L. Reba, and D. Marks. 2012. Measurement of surface energy fluxes from two rangeland sites and comparison with a multilayer canopy model. Journal of Hydrometeorology 13(3):1038-1051, doi: 10.1175/JHM-D-11-093.1.

Flerchinger, G.N., M.L. Reba, T.E. Link, D. Marks. 2015. Modeling Temperature and Humidity Profiles within Forest Canopies. Agricultural and Forest Meteorology 213:251-262.

Fuchs, M., G.S. Campbell and R.I. Papendick. 1978. An analysis of sensible and latent heat

flow in a partially frozen unsaturated soil.   Soil Sci. Soc. Amer. J. 42(3):379-385.

Goudriaan, J.. 1988. The bare bones of leaf-angle distribution in radiation models for canopy
     photosynthesis and energy exchange, Agric. and Forest Meteor., 43:155-169.

Goudriaan, J. 1989. Simulation of micrometeorology of crops, some methods and their problems,
     and a few results.   Agric. and Forest Meteor., 47, 239-258.

Hirota, T., J.W. Pomeroy, R.J. Granger, and C.P. Maule. 2002. An extension of the force-restore
     method to estimating soil temperature at depth and evaluation for frozen soils under snow.
     J. of Geoph. Res. 107(D24), 4767, doi:10.1029/2001JD001280.

Huntingford, C., S.J. Allen, and R.J. Harding. 1995. An intercomparison of single and dual-source
     vegetation-atmosphere transfer models applied to transpiration from Sahelian savanna.
     Boundary-Layer Meteor., 74, 397-418.

Idso, S.B. and R.D. Jackson. 1969.   Thermal radiation from the atmosphere. J. of Geoph. Res.
     74(23):5397-5403.

Idso, S.B., R.D. Jackson, R.J. Reginato, B.A. Kimball and F.S. Nakayama. 1975. The dependence
     of bare soil albedo on soil water content. Journal of Applied Meteorology 14:109-113.
Jarvis, P.G. 1976. The interpretation of the variations in leaf water potential and stomatal
     conductance found in canopies in the field. Philos. Trans. Roy. Soc. London
     B273:593–610.

Kimball, B.A. and E.R. Lemon. 1971. Air turbulence effects upon soil gas exchange. Soil Sci. Soc.
     Amer Proc. 35:126-21

Leuning, R. 2000. Estimation of scalar source/sink distributions in plant canopies using
     Lagrangian dispersion analysis: corrections for atmospheric stability and comparison with
     a multilayer canopy model. Boundary-Layer Meteorology 96:293–314.

Mihailovi_, D.T. and M. Ruml. 1996. Design of land-air parameterization scheme (LAPS) for
     modelling boundary layer surface processes.   Meteor. Atmos. Phys., 58:65-81.

Miller, R.D. 1963. Phase-equilibria and soil freezing. p 193-197 In: International Conference on
     Permafrost. Lafayette, Indiana. National Academy of Science.

Myrold D.D., L.F. Elliot, R.I. Papendick, and G.S. Campbell. 1981. Water potential-water content
     characteristics of wheat straw. Soil Sci. Soc. Amer. Proc. 37:522:527.

Nichols, W.D. 1992. Energy budgets and resistances to energy transport in sparsely vegetated
     rangeland, Agric. and Forest Meteor., 60:221-247.

Norman, J.M. 1979. Modeling the complete crop canopy.   p.249-277 In: B.J. Barfield and J.F.
     Gerber (eds.), Modification of the Aerial Environment of Plants, ASAE Monograph, St.
     Joseph, MI.

Raupach, M.R. 1989. A practical Langrangian method for relating scalar concentrations to source distributions in vegetation canopies. Q.J.R. Meteorol. Soc..115:609-632.

Stewart, J. B. 1988. Modelling surface conductance of pine forest. Agric. For. Meteor. 43:19–35.

Van Bavel, C.H.M., R.J. Lascano, and L. Stroosnijder. 1984. Test and analysis of a model of water use by sorghum. Soil Sci.,137:443-456.

van de Griend, A.A. and J.H. van Boxel. 1989. Water and surface energy balance model with a multilayer canopy representation for remote sensing purposes. Water Resour. Res., 25:949-971.

Zhao, W. and R.J. Qualls. 2005. A multiple-layer canopy scattering model to simulate shortwave radiation distribution within a homogeneous plant canopy, Water Resources Research, 41, W08409, doi:10.1029/2005WR004016.

Appendix 1: Notation

a_c	coefficient for computing matric potential of dead plant canopy elements (m)
a_r	coefficient for computing matric potential of residue elements (m)
a_{sp}	coefficient for computing thermal conductivity of snow (0.021 W m^{-1} C^{-1})
a_α	exponent for calculating albedo of soil surface
A	empirical exponent for relating extinction coefficient $K_{d,j}$ to leaf area index
A_T	weighting coefficient for estimating temperature of bottom soil layer
b	pore-size distribution parameter
b_c	exponent for computing matric potential of dead plant canopy elements
b_r	exponent for computing matric potential of residue elements
b_{sp}	coefficient for computing thermal conductivity of snow (2.51 W m^{-1} C^{-1})
b_v	coefficient accounting for tortuosity in computing vapor diffusion through soil
B	empirical coefficient relating extinction coefficient $K_{d,j}$ to leaf area index
c	solute concentration in soil solution (eq kg^{-1})
c'	solute concentration in soil solution after infiltration event (eq kg^{-1})
c_a	specific heat capacity of air (J kg^{-1} C^{-1})
c_{avg}	average concentration of water entering soil layer during infiltration (eq kg^{-1})
c_c	specific heat capacity of canopy elements (J kg^{-1} C^{-1})
c_i	specific heat capacity of ice (2,100 J kg^{-1} C^{-1})
c_j	specific heat capacity of jth soil constituent (J kg^{-1} C^{-1})
c_l	specific heat capacity of water (4,200 J kg^{-1} C^{-1})
c_r	specific heat capacity of residue elements (J kg^{-1} C^{-1})
c_{sp}	exponent for computing thermal conductivity of snow (2.0)
c_v	exponent accounting for tortuosity in computing vapor diffusion through soil
C	exponent relating extinction coefficient $K_{d\infty}$ to leaf orientation, x
C_1	fractional increase in density per cm load of water equivalent (cm^{-1}h^{-1})
C_2	compaction parameter for snow
C_3	fractional settling of snow at densities less than ρ_d (h^{-1})

C_4	settling parameter for snow (C^{-1})
C_5	ratio of fractional settling rate for wet snow compared to dry snow (h^{-1})
C_c	fraction of cloud cover
C_{L1}	maximum allowable lag for water being routed through the snowpack (h)
C_{L2}	lag-time parameter for for water being routed through the snowpack (cm^{-1})
C_{L3}	recession parameter for water being routed through the snowpack (h)
C_{L4}	attenuation parameter for water being routed through the snowpack (h)
C_r	volumetric heat capacity of residue layer ($J\ m^{-3}\ C^{-1}$)
C_s	volumetric heat capacity of soil ($J\ m^{-3}\ C^{-1}$)
C_v	coefficient for radiation extinction coefficient in snow ($mm^{1/2}\ cm^{-1}$)
d	zero displacement plane for residue or canopy (m) (or derivative funcion)
d_d	damping depth for annual temperature oscillation (m)
d_e	effective zero-plane displacement accounting for a sparse canopy (m)
d_g	zero-plane displacement of ground; set equal to snow depth or zero otherwise (m)
d_l	characteristic dimension of canopy leaves or elements (m)
d_s	grain-size diameter of ice crystals in snow layer (mm)
d_{sp}	depth of snowpack (m)
D_e	effective diffusion coefficient for water vapor in snow ($m^2\ s^{-1}$)
D_H	hydrodynamic dispersion coefficient for solute transport in soil ($m^2\ s^{-1}$)
D_o	molecular diffusion of a given solute in water ($m^2\ s^{-1}$)
D_m	molecular diffusion for solute transport in soil ($m^2\ s^{-1}$)
D_v	effective vapor diffusion coefficient through soil ($m^2\ s^{-1}$)
D_v'	vapor diffusivity in air ($m^2\ s^{-1}$)
E	evaporative flux from system profile ($kg\ s^{-1}\ m^{-2}$)
E_1	parameter for vapor flux enhancement factor
E_2	parameter for vapor flux enhancement factor
E_3	parameter for vapor flux enhancement factor
E_4	parameter for vapor flux enhancement factor
E_5	parameter for vapor flux enhancement factor
E_l	evaporative flux from canopy elements, i.e. leaves ($kg\ s^{-1}\ m^{-2}$)
$E_{l,i,j}$	evaporative flux from canopy elements (leaves) of plant species j within canopy layer i ($kg\ s^{-1}\ m^{-2}$)
f	infiltration rate into soil ($m\ s^{-1}$)
f_*	dimensionless infiltration rate into soil
f_{St}	stomatal restriction factor for solar radiation
f_T	stomatal restriction factor for temperature
f_{VPD}	stomatal restriction factor for vapor pressure deficit
F_*	dimensionless cumulative infiltration into soil layer containing the wetting front
$f_{b,i,\downarrow\downarrow}$	fraction of reflected direct radiation scattered downward
$f_{b,i,\downarrow\uparrow}$	fraction of reflected direct radiation scattered upward
$f_{d,i,\downarrow\downarrow}$	fraction of reflected diffuse radiation scattered forward (e.g. downward radiation scattered downward or upward radiation scattered upward)
$f_{d,i,\downarrow\uparrow}$	fraction of reflected diffuse radiation scattered backward (e.g. downward radiation scattered upward and vice versa)

F_r	fractional area surface cover by flat residue (m^2 m^{-2})
F'_{k+1}	cumulative infiltration water passing through soil layer k (m)
F'_m	cumulative infiltration into soil layer m which contains the wetting front (m)
g	acceleration gravity (9.81 m s^{-2})
G	soil heat flux (W m^{-2})
G_1	empirical coefficient for grain-size diameter (mm)
G_2	empirical coefficient for grain-size diameter (mm)
G_3	empirical coefficient for grain-size diameter (mm)
h_{ce}	effective canopy height accounting for a sparse canopy (m)
h_c	canopy height (m)
h_r	relative humidity expressed as a decimal
H	sensible heat flux from the system profile (W m^{-2})
H_l	sensible heat flux from canopy elements (leaves) to air space within the canopy (W m^{-2})
$H_{l,i,j}$	sensible heat flux from canopy elements (leaves) of plant species j to air space within the canopy layer i (W m^{-2})
k	von Karman constant (taken as 0.4)
k_a	thermal conductivity of still air (0.025 W m^{-1} C^{-1})
k_e	convective transfer coefficient within the canopy air space (m^2 s^{-1})
k_j	thermal conductivity of jth soil constituent (W m^{-1} C^{-1})
k_l	thermal conductivity of liquid water (0.57 W m^{-1} C^{-1})
k_r	effective thermal transfer coefficient (conductive and convective) of residue layer (W m^{-1} C^{-1})
k_{rb}	parameter for influence of wind on vapor transfer through the residue (s m^{-1})
k_{rs}	thermal conductivity of residue material (W m^{-1} C^{-1})
k_s	thermal conductivity of soil (W m^{-1} C^{-1})
k_{sp}	thermal conductivity within snowpack (W m^{-1} C^{-1})
k_t	thermal conductivity of residue layer (W m^{-1} C^{-1})
k_v	convective thermal transfer within the residue layer (W m^{-1} C^{-1})
K	unsaturated soil hydraulic conductivity (m s^{-1})
$K_{b,r}$	extinction coefficient for direct radiation through the residue
$K_{b,j}$	extinction coefficient for direct radiation for plant species j in canopy layer i
K_d	partitioning coefficient between solute absorbed on soil matrix and that in soil solution (kg kg^{-1})
$K_{d,j}$	extinction coefficient of plant species j to diffuse radiation
$K_{d\infty}$	asymptote that $K_{d,j}$ approaches at infinite L_{AI} for a given value of x
$K_{e,m}$	effective conductivity of soil layer containing wetting front (m s^{-1})
$K_{e,k}$	effective conductivity of soil layer k during infiltration (m s^{-1})
K_f	Lagrangian far field dispersion coefficient (m^2 s^{-1})
K_s	saturated soil hydraulic conductivity (m s^{-1})
K_v	convective vapor transfer coefficient within residue layer (m^2 s^{-1})
K_{St}	parameter to control the influence of solar radiation on stomatal resistance (W m^{-2})
K_{VPD}	maximum fractional reduction in stomatal conductance due to vapor pressure deficit

l	pore-connectivity parameter for the Brooks-Corey moisture release curve
L_{clr}	incoming clear-sky long-wave radiation (W m^{-2})
L_f	latent heat of fusion $(335,000 \text{ J kg}^{-1})$
$L_{AI,i,j}$	leaf area index for plant species j in canopy layer i $(\text{m}^2 \text{ m}^{-2})$
$L_{AI,j}$	total leaf area index for plant j
$L_{n,i,j}$	net long-wave radiation for plant species j within canopy layer i (W m^{-2})
L_s	latent heat of sublimation $(2,835,000 \text{ J kg}^{-1})$
L_w	actual lag of excess water being routed through the snowpack (h)
$L_{w,max}$	maximum lag of excess water being routed through the snowpack for present snow conditions (h)
$L_{u,i}$	upward flux of long-wave radiation above canopy layer i
L_v	latent heat of vaporization $(2,500,000 \text{ J kg}^{-1})$
m	empirical exponent in van Genuchten moisture release curve; $m=1-1/n$
$m_{c,i,j}$	biomass of plant j within canopy layer i (kg m^{-2})
m_j	weighting factor for thermal conductivity of jth soil constituent
M_w	molecular weight of water $(0.018 \text{ kg mole}^{-1})$
n	empirical exponent in van Genuchten moisture release curve
n_s	empirical exponent for computing stomatal resistance
n_T	parameter exponent to control temperature influence on stomatal resistance
NC	number of plant canopy layers
NP	number of plant species present in canopy
NS	number of soil layers within soil profile
P	ambient atmospheric pressure (Pa)
q_l	liquid water flux (m s^{-1})
q_v	water vapor flux $(\text{kg m}^{-2} \text{ s}^{-1})$
q_{vp}	soil water vapor flux due to water potential gradient $(\text{kg m}^{-2} \text{ s}^{-1})$
q_{vT}	soil water vapor flux due to temperature gradient $(\text{kg m}^{-2} \text{ s}^{-1})$
r	coefficient for vapor pressure deficit influence on stomatal conductance
r_h	resistance to vapor transfer from residue elements to air within residue layer (s m^{-1})
$r_{h,i,j}$	resistance to convective heat transfer from canopy elements of plant species j within canopy layer i (s m^{-1})
r_H	resistance to convective heat transfer from the surface of system profile (s m^{-1})
$r_{l,i,j}$	leaf resistance to water flow in plant species j within canopy layer i $(\text{m}^3 \text{ s kg}^{-1})$
$r_{r,j,k}$	resistance to water flow through the roots of plant k within soil layer k $(\text{m}^3 \text{ s kg}^{-1})$
r_s	stomatal resistance (s m^{-1})
$r_{s,i,j}$	stomatal resistance of plant species j within canopy layer i (s m^{-1})
r_{so}	stomatal resistance of plant with no water stress (s m^{-1})
r_v	resistance to convective vapor transfer from surface of the system profile (s m^{-1})
$r_{v,i,j}$	resistance to convective vapor transfer from canopy elements of plant species j within canopy layer i (s m^{-1})
r_{vr}	resistance to convective vapor transfer from residue elements and air voids within residue layer (s m^{-1})
R	universal gas constant $(8.3143 \text{ J K}^{-1} \text{ mole}^{-1})$
R_i	gradient Richardson number within the canopy
R_n	net all-wave downward radiation (W m^{-2})

s	atmospheric stability (ratio of thermal to mechanical turbulence)
s_v	slope of the saturated vapor density curve ($d\rho_v'/dT$; kg m^{-3}C^{-1})
S	total solutes present per mass of soil (eq kg^{-1})
S'	total solutes present in soil layer after leaching due to infiltration event (eq kg^{-1})
S_b	direct (beam) solar radiation incident on a horizontal surface(W m^{-2})
$S_{b,i}$	direct solar radiation entering canopy layer i (W m^{-2})
$S_{b,o}$	solar radiation incident on a horizontal surface at the outer edge of the atmosphere (W m^{-2})
S_d	diffuse solar radiation (W m^{-2})
$S_{d,i}$	downward diffuse solar radiation entering canopy layer i (W m^{-2})
$S_{n,i,j}$	net short-wave radiation absorbed by plant type j within canopy layer i
S_o	solar constant (1360 W m^{-2})
S_s	direct solar radiation incident on the local slope (W m^{-2})
S_{sp}	excess water of snowpack in storage (m)
S_t	total solar radiation incident on a horizontal surface (W m^{-2})
$S_{t,i}$	total downward solar radiation above canopy layer i (W m^{-2})
$S_{u,i}$	upward flux of diffuse short-wave radiation above canopy layer i
S_z	net solar radiation flux at a depth z within the snowpack (W m^{-2})
t	time (s)
t'	time since infiltration wetting front entered the current soil layer (s)
t_*	dimensionless time since infiltration wetting front entered the current soil layer
$t_{1/2}$	half-life of solute (d)
T	temperature (C)
T'	temperature of soil layer and water exiting soil layer during infiltration event (C)
T_a	ambient temperature at measured reference height (C)
T_{AVG}	average annual soil surface temperature (C)
T_i	temperature of air within canopy layer i (C)
T_j	total transpiration rate for a given plant species (kg m^{-2} s^{-1})
T_i	temperature of layer i within the system profile (C)
T_{frz}	freezing point of soil water based on water potential of the soil layer (C)
$T_{F,k}$	temperature of infiltration water entering soil layer k (C)
T_H	upper temperature limit for plant transpiration (C)
T_K	temperature (K)
T_L	lower temperature limit for plant transpiration (C)
$T_{l,i,j}$	leaf temperature of plant species j within canopy layer i (C)
T_{Opt}	optimum temperature for plant transpiration (C)
T_{wb}	wet-bulb temperature (C)
u	wind speed at reference height (m s^{-1})
u_g	wind speed at ground surface (m s^{-1})
$u_{c,i}$	wind speed in canopy layer i (m s^{-1})
u_r	wind speed within residue layer (m s^{-1})
u_*	friction velocity (m s^{-1})
U	source/sink term for water flux equation (m^3 m^{-3} s^{-1}).
v	solar radiation extinction coefficient for snow (m^{-1})

V	source/sink term for solute flux (eq kg^{-1} s^{-1})
V_e	coefficient accounting for influence of sparse canopy on momentum transfer
VPD	vapor pressure deficit (kPa)
w_c	gravimetric water content of dead plant canopy material (kg kg^{-1})
w_r	gravimetric water content of residue layer (kg kg^{-1})
w_{sp}	volumetric liquid water content of snow (m^3 m^{-3})
$w_{sp,hold}$	volumetric water holding capacity of snow (m^3 m^{-3})
$w_{sp,max}$	maximum value of $w_{sp,hold}$ (m^3 m^{-3})
$w_{sp,min}$	minimum value of $w_{sp,hold}$ (m^3 m^{-3})
W_o	snowcover outflow (m)
W_L	depth of lagged excess liquid water in the snowpack (m)
W_{sp}	water equivalent of overlying snow (cm)
W_r	dry mass of residue on the surface (kg/m^{-2})
W_x	depth of excess liquid water in the snowpack (m)
x	coefficient relating to leaf orientation ranging from zero for vertically-oriented leaves, to $x = 1$ for random orientation, and to infinity for horizontal leaves
z	vertical distance within system profile (m)
$z*$	dimensionless depth of soil layers above the layer containing the wetting front
z_H	aerodynamic roughness length for heat transfer (m)
z_i	Height above ground surface for canopy layer i
z_m	aerodynamic roughness length for momentum transfer (m)
z_{me}	effective aerodynamic roughness length accounting for a sparse canopy (m)
z_{mg}	aerodynamic roughness length for momentum transfer at ground surface (m)
z_{NS}	depth of bottom soil layer (m)
z_{ref}	reference height above the soil surface for meteorological measurements (m)
α	empirical coefficient in the van Genuchten moisture release curve (m^{-1})
α_d	albedo of dry soil surface
α_s	albedo of soil surface
α_{sp}	albedo of snow surface to diffuse radiation
$\alpha_{sp,ir}$	albedo of snow surface to direct infrared radiation
$\alpha_{sp,v}$	albedo of snow surface to direct radiation in the visible spectrum
$\alpha_{l,b,i}$	effective albedo of canopy layer i to direct radiation
$\alpha_{l,d,i}$	effective albedo of canopy layer i to diffuse radiation
$\alpha_{l,j}$	albedo of leaves or plant elements of plant species j
α_j	albedo of plant species j
β	angle which the sun's rays make with the local slope (rad)
Δt	time increment (s)
$\Delta\theta_l$	change in water content across the infiltration wetting front (m^3 m^{-3})
Δz_k	thickness of soil layer k (m)
ε_{ac}	long-wave emissivity of the atmosphere adjusted for cloud cover
ε_c	clear-sky long-wave emissivity of the canopy elements
ε_{clr}	clear-sky long-wave emissivity of the atmosphere
ε_s	long-wave emissivity of the surface (soil or snow)
ζ	enhancement factor for vapor flux through soil due to temperature gradient

η	weighting factor for end-of-time-step values ($0.5 \leq \eta \leq 1.0$)
θ_a	volumetric air content of soil layer ($m^3\ m^{-3}$)
θ_i	volumetric ice content of soil layer ($m^3\ m^{-3}$)
$\theta_i{}'$	volumetric ice content of soil layer after infiltration event ($m^3\ m^{-3}$)
θ_j	volumetric fraction for j^{th} soil constituent ($m^3\ m^{-3}$)
θ_l	volumetric liquid water content of soil layer ($m^3\ m^{-3}$)
θ_s	volumetric saturated water content of soil layer ($m^3\ m^{-3}$)
θ_s	volumetric saturated water content of soil layer ($m^3\ m^{-3}$)
κ	parameter for hydrodynamic dispersion coefficient (m)
λ	Brooks-Corey pore size distribution parameter
ν	solar radiation extinction coefficient for snow (m^{-1})
π	osmotic potential of soil solution (m)
$\rho_a.$	density of air ($kg\ m^{-3}$)
ρ_b	bulk density of soil ($kg\ m^{-3}$)
ρ_d	density of snow below which the settling rate equals C_3 ($kg\ m^{-3}$)
ρ_e	density of snow at which $w_{sp,hold} = w_{c,\ min}$ ($kg\ m^{-3}$)
ρ_i	density of ice (920 $kg\ m^{-3}$)
ρ_j	density of jth soil constituent ($kg\ m^{-3}$)
ρ_l	density of water (1,000 $kg\ m^{-3}$)
ρ_r	density of residue ($kg\ m^{-3}$)
ρ_{rs}	specific density of residue ($kg\ m^{-3}$)
ρ_{sp}	density of ice portion of snowpack ($kg\ m^{-3}$)
ρ_v	vapor density of air space ($kg\ m^{-3}$)
$\rho_v{}'$	saturated vapor density ($kg\ m^{-3}$)
ρ_{va}	ambient vapor density at reference height ($kg\ m^{-3}$)
$\rho_{v,i}$	vapor density of air within canopy layer i ($kg\ m^{-3}$)
ρ_{vs}	vapor density at an exchange surface ($kg\ m^{-3}$)
$\rho_{vs}{}'$	saturated vapor density at an exchange surface ($kg\ m^{-3}$)
σ_w	standard deviation of the vertical velocity ($m\ s^{-1}$)
τ	molecular diffusion coefficient for accounting for soil tortuosity
$\tau_{b,i}$	transmissivity to direct (beam) radiation for canopy layer i
$\tau_{b,i,j}$	transmissivity of direct (beam) radiation in canopy layer i based on leaf area of plant species j
$\tau_{b,r}$	transmissivity to direct (beam) radiation within the residue layer
τ_d	atmospheric diffuse solar radiation transmission coefficient ($S_t\ /S_{b,o}$)
$\tau_{d,i}$	transmissivity to diffuse radiation for canopy layer i
$\tau_{d,i,j}$	transmissivity of diffuse radiation in canopy layer i based on leaf area of plant species j
$\tau_{d,r}$	transmissivity to diffuse radiation within the residue layer
τ_l	Lagrangian time scale (s)
$\tau_{l,b,i}$	effective leaf transmittance of canopy layer i to direct radiation
$\tau_{l,d,i}$	effective leaf transmittance of canopy layer i to diffuse radiation
$\tau_{l,j}$	transmittance of leaves or plant elements of plant species j
τ_t	atmospheric total solar radiation transmissivity of the atmosphere ($S_t\ /S_{b,o}$)

$\tau_{t.\max}$	maximum clear-sky solar transmissivity of the atmosphere
φ_h	stability function for heat transfer within the canopy
φ_H	diabatic correction factor for thermal transfer
φ_w	stability function for momentum transfer within the canopy
ϕ	total water potential (m)
ϕ_s	sun's altitude angle above the horizon (rad)
ψ	soil or residue water potential (m)
ψ_e	soil air-entry potential (m)
ψ_c	critical leaf water potential at which stomatal resistance is twice its minimum value (m)
ψ_f	suction head of soil below the infiltration wetting front (m)
ψ_k	water potential of soil layer k (m)
ψ_l	leaf water potential (m)
$\psi_{l,i,j}$	leaf water potential of plant species j within canopy layer i (m)
ψ_H	diabatic temperature profile correction for heat transfer
ψ_m	diabatic wind speed profile correction for momentum transfer
$\psi_{x,j}$	xylem water potential of plant species j (m)
ω	radial frequency of annual temperature oscillation (1.99238×10^{-7} s^{-1})
Ω_j	clumping factor to account for the fact that leaves are less efficient at intercepting radiation when clumped together compared to being uniformly distributed